

# Tropical Gradient Descent

Roan Talbut<sup>1,†</sup> and Anthea Monod<sup>1</sup>

**1 Department of Mathematics, Imperial College London, UK**

† Corresponding e-mail: [r.talbut21@imperial.ac.uk](mailto:r.talbut21@imperial.ac.uk)

## Abstract

We propose a gradient descent method for solving optimisation problems arising in settings of tropical geometry—a variant of algebraic geometry that has become increasingly studied in applications such as computational biology, economics, and computer science. Our approach takes advantage of the polyhedral and combinatorial structures arising in tropical geometry to propose a versatile approach for approximating local minima in tropical statistical optimisation problems—a rapidly growing body of work in recent years. Theoretical results establish global solvability for 1-sample problems and a convergence rate of  $O(1/\sqrt{k})$ . Numerical experiments demonstrate the method’s superior performance over classical descent for tropical optimisation problems which exhibit tropical convexity but not classical convexity. Notably, tropical descent seamlessly integrates into advanced optimisation methods, such as Adam, offering improved overall performance.

**Keywords:** tropical quasi-convexity; tropical projective torus; gradient descent; phylogenetics.

## 1 Introduction

Where algebraic geometry studies geometric properties that can be expressed algebraically of solution sets of systems of multivariate polynomials, *tropical geometry* restricts to the case of polynomials defined by linearising operations, where the sum of two elements is their maximum and the product of two elements is their sum. Evaluating polynomials with these operations results in piecewise linear functions. Tropical geometry is a relatively young field of pure mathematics established in the 1990s (with roots dating back further) and has recently become an area of active interest in computational and applied mathematics for its relevance to the problem of dynamic programming in computer science (Maclagan & Sturmfels (2021)); in mechanism design for two-player games in game theory (Lin & Tran (2019)); and statistical analyses of phylogenetic trees (Monod *et al.* (2022)). Given the connection of tropical geometry to applied sciences, developing and implementing computational techniques for tropical geometric settings is becoming increasingly important.

A central task to a vast majority of computational tasks and training machine learning models entails solving an optimisation problem. In this paper, we are motivated by the optimisation problems in statistics in tropical geometric settings. We focus on the classical gradient descent approach for optimisation and adapt it to the setting of tropical geometry. We thus provide a unifying gradient descent framework to solve the optimisation problems entailed in the computation of a wide range of statistical quantities and methods in tropical spaces which are an area of active interest in applied tropical geometry.

The remainder of this paper is organised as follows. The following section contains the necessary foundations of tropical geometry to present, an introduction to tropical location problems functions (Comănesci (2023)), and the array of statistical optimisation tasks studied in this paper. In Section 3 we formulate steepest descent with respect to the tropical norm and present the theoretical guarantees for tropical descent, most notably its convergence for a wide class of tropically quasi-convex functions and a convergence rate of  $O(1/\sqrt{k})$ . In Section 4, we perform a comprehensive numerical study of our proposed tropical gradient descent method and its performance in the statistical optimisation problems of interest. We conclude with a discussion of possible future work on tropical gradient methods in Section 5.

## 2 Background and Preliminaries

In this section, we overview the background on tropical geometry and present the statistical concepts and methodologies which are defined by an optimisation problem that we will study in the tropical setting.

### 2.1 Tropical Geometry

Here, we review the algebraic and geometric structure of the tropical projective torus, the state space for phylogenetic data and the domain of our tropical statistical optimisation problems.

**Definition 1** (Tropical Algebra). The *tropical algebra* is the semiring  $\overline{\mathbb{R}} = \mathbb{R} \cup \{-\infty\}$  with the addition and multiplication operators—tropical addition and tropical multiplication, respectively—given by

$$a \boxplus b = \max\{a, b\}, \quad a \odot b = a + b.$$

The additive identity is  $-\infty$  and the multiplicative identity is 0. Tropical subtraction is not defined; tropical division is given by classical subtraction.

The tropical algebra defined above is sometimes referred to as the *max-plus algebra*; we can define the min-plus algebra analogously, taking  $\min\{a, b\} =: a \oplus b$  as the additive operation on  $\mathbb{R} \cup \{\infty\}$ . These are algebraically equivalent through negation. Unless specified, we use the max-plus convention as this is better suited for phylogenetic statistics on the tropical projective torus (Speyer & Sturmfels, 2004).

**Definition 2** (Tropical Projective Torus). The  $n$ -dimensional *tropical projective torus* is a quotient space constructed by endowing  $\mathbb{R}^{n+1}$  with the equivalence relation

$$\mathbf{x} \sim \mathbf{y} \Leftrightarrow \exists a : \mathbf{x} = a \odot \mathbf{y}; \tag{1}$$

it is denoted by  $\mathbb{R}^{n+1}/\mathbb{R}\mathbf{1}$ . The generalised Hilbert projective metric, also referred to as the *tropical metric*, is given by

$$d_{\text{tr}}(\mathbf{x}, \mathbf{y}) = \max_i \{x_i - y_i\} - \min_i \{x_i - y_i\} = \max_{i,j} \{x_i - y_i - x_j + y_j\}.$$

This metric is induced by the tropical norm, which is given by

$$\|\mathbf{x}\|_{\text{tr}} = \max_i x_i - \min_i x_i.$$

The tropical projective torus is the ambient space containing the tropical Grassmannian, which is equivalent to the space of phylogenetic trees (Speyer & Sturmfels (2004)). This has sparked the study of tropical data science, formalising statistical techniques which respect the tropical geometry of the state space (Monod *et al.* (2018); Yoshida (2020)).

The metric above is widely accepted and preferred for the development of geometric statistical tools on the tropical projective torus (Yoshida (2020)). However, recent work has shown theoretical advantages to the use of an asymmetric metric (Comăneci & Joswig (2023)).

**Definition 3** (Tropical Asymmetric Distance). The *tropical asymmetric distance* on  $\mathbb{R}^n/\mathbb{R}\mathbf{1}$  is given by

$$d_{\Delta_{\min}}(\mathbf{a}, \mathbf{b}) := \sum_i (b_i - a_i) - n \min_j (b_j - a_j),$$

$$d_{\Delta_{\max}}(\mathbf{a}, \mathbf{b}) := n \max_j (b_j - a_j) - \sum_i (b_i - a_i).$$

*Remark 4.* The asymmetric distances act as an  $\ell_1$  norm on the tropical projective torus, which the symmetric metric  $d_{\text{tr}}$  acts as an  $\ell_\infty$  norm. We note that  $nd_{\text{tr}} = d_{\Delta_{\min}} + d_{\Delta_{\max}}$ . Figure 1 shows the balls for each tropical metric of interest.

We now define the primary geometric objects of interest in the tropical projective torus; hyperplanes, lines, and convex hulls. We use the max-convention for these definitions, though we note each has a min-convention equivalent.

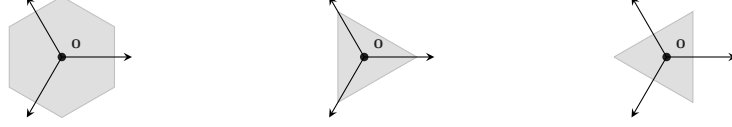


Figure 1: The  $d_{\text{tr}}$ ,  $d_{\Delta_{\min}}$  and  $d_{\Delta_{\max}}$  tropical unit balls in  $\mathbb{R}^3/\mathbb{R}\mathbf{1} \cong \mathcal{H} = \{\sum x_i = 0\}$ .

**Definition 5** (Tropical Hyperplanes). The *tropical hyperplane*  $\mathcal{H}_{\mathbf{a}}$  defined by the linear form  $a_1 \odot x_1 \boxplus \dots \boxplus a_n \odot x_n$  is given by

$$\mathcal{H}_{\mathbf{a}} = \{\mathbf{x} : \exists i \neq j \text{ s.t. } a_i + x_i = a_j + x_j = \max\{a_k + x_k\}\}.$$

**Definition 6** (Tropical Line Segments). For any two points  $\mathbf{a}, \mathbf{b} \in \mathbb{R}^n/\mathbb{R}\mathbf{1}$ , the *tropical line segment* between  $\mathbf{a}$  and  $\mathbf{b}$  is the set

$$\gamma_{\mathbf{ab}} = \{\alpha \odot \mathbf{a} \boxplus \beta \odot \mathbf{b} \mid \alpha, \beta \in \mathbb{R}\}$$

with tropical addition taken coordinate-wise.

Tropical line segments define a unique geodesic path between any two points, but general geodesics are not uniquely defined on the tropical projective torus.

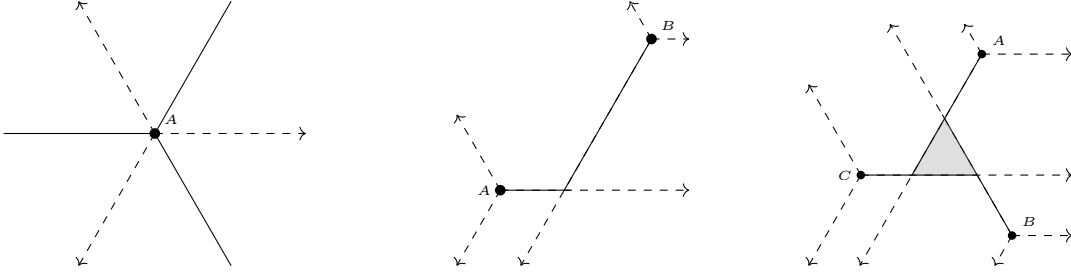


Figure 2: A tropical hyperplane, tropical line segment and tropical convex hull in  $\mathbb{R}^3/\mathbb{R}\mathbf{1} \cong \mathcal{H} = \{\mathbf{x} : \sum x_i = 0\}$ . The dashed lines show coordinate directions.

**Definition 7** (Tropical Convex Hulls (Develin & Sturmfels, 2004)). A set  $S$  is *max-tropically convex* if it contains  $\alpha \odot \mathbf{x} \boxplus \beta \odot \mathbf{y}$  for all  $\mathbf{x}, \mathbf{y} \in S$  and  $\alpha, \beta \in \mathbb{R}$ . For a finite subset  $X = \{\mathbf{x}_1, \dots, \mathbf{x}_n\} \subset \mathbb{R}^n/\mathbb{R}\mathbf{1}$ , the *max-plus tropical convex hull* of  $X$  is the set of all max-tropical linear combinations of points in  $X$ ,

$$\text{tconv}_{\max}(X) = \{\alpha_1 \odot \mathbf{x}_1 \boxplus \alpha_2 \odot \mathbf{x}_2 \boxplus \dots \boxplus \alpha_n \odot \mathbf{x}_n \mid \alpha_1, \dots, \alpha_n \in \mathbb{R}\}.$$

Similarly, the *min-tropical convex hull* of  $X$ ,  $\text{tconv}_{\min}(X)$  is the set of all min-tropical linear combinations of points in  $X$ .

A study of tropically convex functions requires an understanding of both max-tropical and min-tropical convex hulls, as we will see in our following consideration of tropical location problems.

## 2.2 Tropical Location Problems

Tropical location problems are a new avenue of research, motivated by the optimisation of statistical loss functions; they involve the minimisation over some dataset of some loss function which heuristically increases with distance from some kernel. Here we outline the relevant definitions of tropical location problems and their theoretical behaviour as presented by Comănesci (2023). We introduce the problem of tropical linear regression (Akian *et al.* (2023)) as motivation.

### 2.2.1 Motivating Example

The problem of tropical linear regression looks to find the best-fit tropical hyperplane which minimises the maximal distance to a set of data points. While this is an inherently statistical optimisation problem, Akian *et al.* (2023) prove it to be polynomial-time equivalent to solving mean payoff games.

A tropical hyperplane is uniquely defined by a cone point  $\mathbf{t} \in \mathbb{R}^N/\mathbb{R}\mathbf{1}$ , allowing us to formulate the best-fit tropical hyperplane as an optimisation problem over  $\mathbb{R}^N/\mathbb{R}\mathbf{1}$ .

**Definition 8** (Tropical Linear Regression (Akian *et al.* (2023))). Let  $X = \{\mathbf{x}_1, \dots, \mathbf{x}_K\} \subset \mathbb{R}^N/\mathbb{R}\mathbf{1}$  be our dataset. The *tropical linear regression problem* finds the vertex  $\mathbf{t} \in \mathbb{R}^N/\mathbb{R}\mathbf{1}$  of the best-fit hyperplane:

$$\min_{\mathbf{t} \in \mathbb{R}^N/\mathbb{R}\mathbf{1}} f(\mathbf{t}) = \max_{k \leq K} d_{\text{tr}}(\mathbf{x}, \mathcal{H}_{\mathbf{t}}) = \max_{k \leq K} (\mathbf{x}_k - \mathbf{t})_i - (\mathbf{x}_k - \mathbf{t})_j$$

where  $i, j$  are such that  $\forall \ell \neq i, j : (\mathbf{x}_k - \mathbf{t})_i \geq (\mathbf{x}_k - \mathbf{t})_j \geq (\mathbf{x}_k - \mathbf{t})_\ell$ .

In Figure 3, we see a heatmap of this objective function over the tropical projective plane. We see immediately that the objective is not convex. The linear regression objective has sparse gradient almost everywhere, which produces valleys. These properties are considered unfavourable extreme cases for gradient methods, but are particularly common in tropical optimisation problems. While the tropical linear regression problem is not convex, it is quasi-convex along tropical line segments; that is, its sub-level sets are tropically convex.

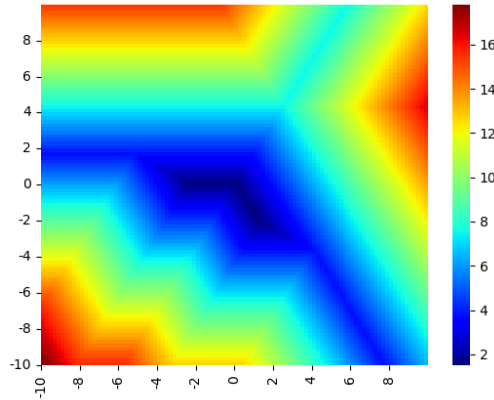


Figure 3: A heat map of a 3-sample linear regression objective on  $\mathbb{R}^3/\mathbb{R}\mathbf{1} \cong \mathcal{H} = \{\mathbf{x} : \sum x_i = 0\}$ .

### 2.2.2 $\Delta$ -Star Quasi-Convexity

In formalising tropical location problems, Comănesci (2023) first considers functions which increase along tropical geodesics from a kernel  $\mathbf{v}$ ; that is, for any point  $\mathbf{t}$  on a geodesic from  $\mathbf{v}$  to  $\mathbf{w}$ , we have that  $f(\mathbf{t}) \leq f(\mathbf{w})$ . This property is equivalent to star-convexity of sublevel sets. To formally state this, we define (oriented) geodesic segments and  $\Delta_{\min}$ -star convexity of sets.

**Definition 9** (Oriented Geodesic Segment). The (oriented) geodesic segment between  $\mathbf{a}, \mathbf{b} \in \mathbb{R}^n/\mathbb{R}\mathbf{1}$ , is given by  $[\mathbf{a}, \mathbf{b}]_{\Delta_{\max}} := \{\mathbf{x} \in \mathbb{R}^n/\mathbb{R}\mathbf{1} : d_{\Delta_{\max}}(\mathbf{a}, \mathbf{x}) + d_{\Delta_{\max}}(\mathbf{x}, \mathbf{b}) = d_{\Delta_{\max}}(\mathbf{a}, \mathbf{b})\}$ .

**Definition 10** ( $\Delta_{\min}$ -Star Convex Set). A set  $K \subseteq \mathbb{R}^n/\mathbb{R}\mathbf{1}$  is a  $\Delta_{\max}$ -star-convex set with kernel  $\mathbf{v}$  if, for every  $\mathbf{w} \in K$ , we have  $[\mathbf{v}, \mathbf{w}]_{\Delta_{\max}} \subseteq K$ .

Using the above definitions, we can characterise a loss function which is increasing along tropical geodesics as a function with  $\Delta_{\max}$ -star-convex sublevel sets. The following definition gives a closed form expression for such functions, while Theorem 12 proves their equivalence.

**Definition 11** (Comăneci (2023)). A function  $f : \mathbb{R}^n / \mathbb{R}\mathbf{1} \rightarrow \mathbb{R}$  is  $\Delta_{\max}$ -star-quasi-convex with kernel  $\mathbf{v}$  if  $f(\mathbf{x}) = \hat{\gamma}(\mathbf{x} - \mathbf{v})$  for some increasing  $\gamma : \mathbb{R}_{\geq 0}^n \rightarrow \mathbb{R}$ , where  $\hat{\gamma}(\mathbf{x}) = \gamma((\max_i x_i)\mathbf{1} - \mathbf{x})$ .

**Theorem 12** (Theorem 17, Comăneci (2023)). A continuous function  $f : \mathbb{R}^n / \mathbb{R}\mathbf{1} \rightarrow \mathbb{R}$  is  $\Delta_{\max}$ -star-quasi-convex with kernel  $\mathbf{v}$  if and only if all of its non-empty sub-level sets are  $\Delta_{\max}$ -star convex with kernel  $\mathbf{v}$ .

These  $\Delta_{\max}$ -star-convex functions act as a loss function with respect to a single datapoint. For example, the tropical metric  $d_{\text{tr}}$  is both  $\Delta_{\min}$  and  $\Delta_{\max}$ -star-quasi-convex. The distance to a hyperplane  $d_{\text{tr}}(\mathbf{x}, \mathcal{H}_{\mathbf{t}})$  is  $\Delta_{\max}$ -star-quasi-convex in  $\mathbf{x}$ , but  $\Delta_{\min}$ -star-quasi-convex in  $\mathbf{t}$ .

As a final remark, we note that  $\Delta_{\max}$ -star-quasi-convex functions are a special case of tropically quasi-convex functions by the following lemma. We limit our theoretical considerations to  $\Delta_{\max}$ -star-quasi-convex functions to utilise their closed form expression given in Definition 11, however numerical experiments demonstrate strong performance for more general tropical quasi-convex functions.

**Lemma 13** (Comăneci (2023)). Any  $\Delta_{\max}$ -star-convex set is max-tropically convex. Hence, any  $\Delta_{\max}$ -star-quasi-convex function is tropically quasiconvex in that it has tropically convex sublevel sets.

### 2.2.3 Tropical Location Problems

The  $\Delta$ -star-convex functions defined above are generally a measure of closeness to the kernel  $\mathbf{v}$ , but in minimising a statistical loss function we look at closeness to a sample of points. A *location problem* (Laporte *et al.* (2019)) measures the closeness to a sample rather than a single kernel.

**Definition 14** (Max(/min)-tropical location problem (Comăneci (2023))). Consider a dataset  $X = \{\mathbf{x}_1, \dots, \mathbf{x}_K\} \subset \mathbb{R}^n / \mathbb{R}\mathbf{1}$ . For  $k \leq K$ , let  $h_k$  be a  $\Delta_{\max}$ -star-quasi-convex function with kernel  $\mathbf{x}_k$ , and let  $g : \mathbb{R}^m \rightarrow \mathbb{R}$  be an increasing function. A *max-tropical location problem* is the minimisation of an objective function  $f : \mathbb{R}^n / \mathbb{R}\mathbf{1} \rightarrow \mathbb{R}$  given by  $h = g(h_1, \dots, h_m)$ . A *min-tropical location problem* is defined similarly, where the  $h_k$  are  $\Delta_{\min}$ -star-quasi-convex.

The main result by Comăneci (2023) is the following; tropical location problems contain a minimum in the tropical convex hull of its dataset  $X$ .

**Theorem 15** (Theorem 20, Comăneci (2023)). Let  $f$  be the objective function of a max-tropical location problem. Then there is a minimum of  $f$  belonging to  $\text{tconv}_{\min}(X)$ . Conversely, min-tropical location problems have minima belonging to  $\text{tconv}_{\max}(X)$ .

We can now revisit our motivating example (Definition 8), showing that tropical linear regression is not just a min-tropical location problem, but also demonstrates tropical quasi-convexity.

**Proposition 16.** The tropical linear regression problem is a tropically quasi-convex min-tropical location problem.

*Proof.*

$$\begin{aligned} f(\mathbf{t}) &= \max_{k \leq K} \min_j [\max_i [x_{ki} - t_i] - x_{kj} + t_j] \\ &= \max_{k \leq K} \min_j [t_j - x_{kj} - \min_i [t_i - x_{ki}]] \end{aligned}$$

These are min-tropical location problems with:

$$\begin{aligned} g(\mathbf{h}) &= \max_{k \leq K} h_k, \\ h_k(\mathbf{t}) &= \hat{\gamma}(\mathbf{t} - \mathbf{x}_k), \\ \gamma(\mathbf{t}) &= \min_j t_j. \end{aligned}$$

This  $g$  and  $\gamma$  are increasing and each  $h_k$  has kernel  $x_k$ , satisfying the conditions for a min-tropical location problem.

As the  $h_k$  are  $\Delta_{\min}$ -star-convex, their sublevel sets are min-tropically convex. This is preserved when taking a maximum over samples, so  $f$  also has min-tropically convex sublevel sets.  $\square$

As mentioned in Lemma 13,  $\Delta_{\min}$ -star-quasi-convexity implies tropical quasi-convexity. However, the tropical linear regression problem is a case in which the reverse implication does not hold; for any sample of size  $\geq 1$ , the linear regression loss function is not  $\Delta_{\min}$ -star-quasi-convex.

## 2.3 Tropical Data Science

We now review various tropical statistical optimisation problems which have been introduced in the literature in recent years, and which are used to test our tropical descent methodology. We note the varying degrees of convexity demonstrated by each of them.

These statistical concepts and methods showcase the breadth of applicability of our proposed methodology: optimisation is a central task in computing important statistical quantities, tasks in both descriptive and inferential statistics, and distances between probability measures. Adapting these statistical tasks to the setting of tropical geometry is not straightforward and it is not immediate that a single tropical optimisation method can be used to find solutions to the optimisation problems.

### 2.3.1 Centrality Statistics

Our first problems of interest, Fermat–Weber Points and Fréchet means, are centrality statistics for data on a general metric space; Fermat–Weber points (Wesolowsky (1993)) act as a generalised median, while Fréchet means (Fréchet (1948)) are a generalisation of the mean.

**Definition 17** (Tropical Fermat–Weber Points (Lin & Yoshida (2018))). Let  $X = \{\mathbf{x}_1, \dots, \mathbf{x}_K\} \subset \mathbb{R}^N/\mathbb{R}\mathbf{1}$  be our dataset. A solution to the following optimisation problem is a *tropical Fermat–Weber point*:

$$\min_{\mathbf{t} \in \mathbb{R}^N/\mathbb{R}\mathbf{1}} f(\mathbf{t}) = \frac{1}{K} \sum_{k \leq K} d_{\text{tr}}(\mathbf{x}_k, \mathbf{t}).$$

**Definition 18** (Tropical Fréchet means (Jazlan *et al.* (2024+); Monod *et al.* (2022))). Let  $X = \{\mathbf{x}_1, \dots, \mathbf{x}_K\} \subset \mathbb{R}^N/\mathbb{R}\mathbf{1}$  be our dataset. A solution to the following optimisation problem is a *tropical Fréchet mean*:

$$\min_{\mathbf{t} \in \mathbb{R}^N/\mathbb{R}\mathbf{1}} f(\mathbf{t}) = \left[ \frac{1}{K} \sum_{k \leq K} d_{\text{tr}}(\mathbf{x}_k, \mathbf{t})^2 \right]^{1/2}.$$

The Fermat–Weber and Fréchet mean problems are both max-tropical and min-tropical location problems, as the tropical metric  $d_{\text{tr}}$  is both  $\Delta_{\min}$  and  $\Delta_{\max}$ -star-quasiconvex. In fact, they are both classically convex and hence act as a benchmark against which we will test our gradient methods.

### 2.3.2 Wasserstein Projections

The next statistical optimisation problem was motivated by Cai & Lim (2022), and looks to identify a tropical projection which minimises the Wasserstein distance between samples in different tropical projective torii.

**Definition 19** (Tropical Wasserstein Projections (Talbut *et al.* (2023))). Let  $X = \{\mathbf{x}_1, \dots, \mathbf{x}_K\} \subset \mathbb{R}^N/\mathbb{R}\mathbf{1}$ ,  $Y = \{\mathbf{y}_1, \dots, \mathbf{y}_K\} \subset \mathbb{R}^M/\mathbb{R}\mathbf{1}$  be our datasets. Let  $J_1, \dots, J_M$  be a non-empty partition of  $[N]$ . Then the *tropical  $p$ -Wasserstein projection problem* is the minimisation of the following objective function:

$$\min_{\mathbf{t} \in \mathbb{R}^N/\mathbb{R}\mathbf{1}} f_p(\mathbf{t}) = \left( \frac{1}{K} \sum_{k \leq K} \left\| [\max_{i \in J_j}(\mathbf{x}_k + \mathbf{t})]_j - \mathbf{y}_k \right\|_{\text{tr}}^p \right)^{1/p}$$

The *tropical  $\infty$ -Wasserstein projection problem* is the minimisation of:

$$\min_{\mathbf{t} \in \mathbb{R}^N/\mathbb{R}\mathbf{1}} f_{\infty}(\mathbf{t}) = \max_{k \leq K} \left\| [\max_{i \in J_j}(\mathbf{x}_k + \mathbf{t})]_j - \mathbf{y}_k \right\|_{\text{tr}}$$

In contrast to the work by Lee *et al.* (2021) which looks to solve the optimal transport problem for intrinsic measures on  $\mathbb{R}^n/\mathbb{R}\mathbf{1}$ , this  $p$ -Wasserstein projection problem is computing an optimal projection for empirical samples.

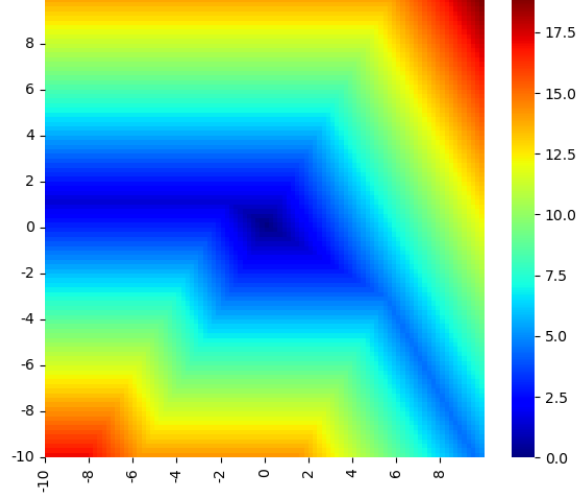


Figure 4: A heat map of a 3-sample  $\infty$ -Wasserstein projection objective on  $\mathbb{R}^3/\mathbb{R}\mathbf{1} \cong \mathcal{H} = \{\mathbf{x} : \sum x_i = 0\}$ .

**Proposition 20.** *The tropical  $p, \infty$ -Wasserstein projections are max-tropical location problems, and the  $\infty$ -Wasserstein projection has max-tropically convex sublevel sets.*

*Proof.* Let  $\mathbf{z}_k = (x_{ki} - y_{kj})_{i \leq N}$  where  $j$  is such that  $i \in J_j$ . We then have that

$$\begin{aligned} \|[\max_{i \in J_j}(\mathbf{x}_k + \mathbf{t})]_i - \mathbf{y}_k\|_{\text{tr}} &= \max_l [t_l + z_{kl}] + \max_j [\min_{i \in J_j} -t_i - z_{ki}] \\ &= \max_j [\min_{i \in J_j} [\max_l [t_l + z_{kl}] - t_i - z_{ki}]] \end{aligned}$$

The  $p, \infty$ -Wasserstein projections can then be written as

$$\begin{aligned} f_p(\mathbf{t}) &= \left( \frac{1}{K} \sum_{k \leq K} \left( \max_j [\min_{i \in J_j} [\max_l [t_l + z_{kl}] - t_i - z_{ki}]] \right)^p \right)^{1/p} \\ f_\infty(\mathbf{t}) &= \max_{k \leq K} \max_j [\min_{i \in J_j} [\max_l [t_l + z_{kl}] - t_i - z_{ki}]] \end{aligned}$$

These are max-tropical location problems with:

$$\begin{aligned} g_p(\mathbf{h}) &= \left( \frac{1}{K} \sum_{k \leq K} h_k^p \right)^{1/p}, \\ g_\infty(\mathbf{h}) &= \max_{k \leq K} h_k, \\ h_k(\mathbf{t}) &= \hat{\gamma}(\mathbf{t} + \mathbf{z}_k), \\ \gamma(\mathbf{t}) &= \max_j \min_{i \in J_j} t_i. \end{aligned}$$

The  $g_p, g_\infty$  and  $\gamma$  are increasing and each  $h_k$  has kernel  $-z_k$ , satisfying the conditions for a max-tropical location problem.

As the  $h_k$  are  $\Delta_{\max}$ -star-convex, their sublevel sets are max-tropically convex. This is preserved when taking a maximum over samples, so  $f_\infty$  also has max-tropically convex sublevel sets.  $\square$

### 3 Steepest Descent with the Tropical Norm

This section comprises the theoretical contributions of this paper; we outline our proposed method of tropical descent, and the theoretical convergence guarantees for tropical descent when applied to tropical location problems.

We treat optimisation over  $\mathbb{R}^N/\mathbb{R}\mathbf{1}$  as optimisation over  $\mathbb{R}^N$  with the knowledge that  $f$  is constant along  $\mathbf{1}$ -rays. We assume that for all  $\mathbf{t}$ , we can compute some gradient  $\nabla f(\mathbf{t})$  which is contained in the *generalised Clarke derivative* of  $\mathbf{t}$ .

**Definition 21** (Generalised Clarke Derivative (2.13, I.I of Kiwiel (2006))). We define the set  $M_f(\mathbf{t})$  by

$$M_f(\mathbf{t}) = \{\mathbf{z} \in \mathbb{R}^N : \nabla f(\mathbf{y}_l) \rightarrow \mathbf{z}, \text{ where } \mathbf{y}_l \rightarrow \mathbf{t}, f \text{ differentiable at each } \mathbf{y}_l\}.$$

Then the *generalised Clarke derivative* is given by

$$\partial f(\mathbf{t}) = \text{conv } M_f(\mathbf{t}).$$

#### 3.1 Proposed Method

In defining tropical descent, we refer back to the motivation behind classical gradient descent; that is, the steepest descent direction.

**Definition 22** (Steepest Descent Direction (Boyd & Vandenberghe (2004))). A normalised *steepest descent direction* with respect to the norm  $\|\cdot\|$  is:

$$\mathbf{d} = \text{argmax}\{\nabla f(\mathbf{t})^\top \mathbf{v} : \|\mathbf{v}\| = 1\}.$$

With respect to the Euclidean norm, the normalised gradient is a steepest descent direction. When we use a the tropical norm, the steepest descent directions are characterised by the following lemma.

**Lemma 23.** *Suppose  $\nabla f \neq 0$ . Then direction  $\mathbf{v}$  is a normalised tropical steepest descent direction iff*

$$\begin{aligned} v_i = 1 &\Leftrightarrow \nabla f_i < 0 \\ v_i = 0 &\Leftrightarrow \nabla f_i > 0 \end{aligned}$$

*Proof.* WLOG, we assume  $0 \leq v_i \leq 1$ . Then

$$\nabla f^\top \mathbf{v} \leq \sum_{\nabla f_i > 0} \nabla f_i$$

This is achieved if and only if  $v_i = 1$  for all  $i$  such that  $\nabla f_i > 0$ , and  $v_i = 0$  for all  $i$  such that  $\nabla f_i < 0$ . We note that any such  $v_i$  satisfies  $\|\mathbf{v}\|_{\text{tr}} = 1$  as  $\sum \nabla f_i = 0, \nabla f_i \neq 0$ , and hence  $\nabla f_i$  has positive and negative coordinates.  $\square$

This lemma uniquely defines  $\mathbf{d}$  if and only if, for every coordinate  $i$ ,  $\nabla f_i \neq 0$ . To uniquely define a descent direction for any  $\mathbf{x}$ , we take the direction  $\mathbf{d}$  given by

$$d_i = \begin{cases} 1 & \text{if } \nabla f_i > 0, \\ 0 & \text{otherwise.} \end{cases}$$

We refer to this as a *positive descent* direction. In contrast,

$$d_i = \begin{cases} -1 & \text{if } \nabla f_i < 0, \\ 0 & \text{otherwise.} \end{cases}$$

defines a *negative descent* direction.

Throughout the rest of this paper, we use the positive descent direction as convention, and will specify when the negative descent direction is used instead. Tropical descent therefore refers to the method outlined by Algorithm 1, for some specified step size rule, while we refer to classical gradient descent as classical descent.



---

**Algorithm 1** Tropical Descent

---

```
for  $n < \text{max\_steps}$  do
   $\mathbf{g}_n \leftarrow \nabla f(\mathbf{t}_{n-1});$ 
   $\mathbf{d}_n \leftarrow [\mathbf{g}_n > 0]_{i \leq N};$ 
   $\mathbf{t}_n \leftarrow \mathbf{t}_{n-1} - a_n \mathbf{d}_n;$ 
```

---

### 3.2 Convergence Guarantees

In this section we prove the theoretical guarantees of tropical descent for max-tropical location problems. We show that tropical descent must converge to the tropical convex hull of the data, and hence will necessarily find a minimum of a  $\Delta_{\max}$ -star-convex problem. Throughout this section, we assume the step sizes  $a_n$  satisfy  $a_n \rightarrow 0, \sum a_n = \infty$ .

We first highlight the key difference in stability between classical descent and tropical descent; if some component of the gradient is locally zero, tropical descent cannot converge in that neighbourhood.

**Proposition 24.** *Assume that for all  $n$ ,  $\nabla f(\mathbf{t}_n) \neq \mathbf{0}$ . Suppose in some bounded open  $U$ ,  $\nabla f_i$  is identically 0. Then no point in  $\text{int } U$  is a convergence point for  $\mathbf{t}_n$ ; in particular, if  $\mathbf{t}_m \in U$  we will eventually leave  $U$ .*

*Proof of Proposition 24.* Assume otherwise. Then for all  $n \geq m$ , we have  $\nabla f(\mathbf{t}_n)_i = 0$ , so  $t_{ni}$  is constant. At each step, we decrease at least one coordinate by  $a_n$ , so as  $n \rightarrow \infty$ :

$$\sum_j t_{nj} \leq \sum_j t_{mj} - \sum_{n \geq m} a_n \rightarrow -\infty.$$

Therefore  $\|\mathbf{t}_n\|_{\text{tr}}$  will become arbitrarily large, as  $\min_j t_{nj} \rightarrow -\infty$  while  $\max_j t_{nj} \geq t_{ni}$ . Then we must have left  $U$ ; contradiction.  $\square$

As a result, local minima such as the valleys in figures 4 and 3 can be stable with respect to classical descent but unstable with respect to tropical descent. We next prove an opposing result; tropical gradient descent must converge to the tropical convex hull of the data points. This result stems from the following observation on the gradient of  $\Delta_{\max}$ -star-quasi-convex functions.

*Remark 25.* We note that for a  $\Delta_{\max}$ -star-quasi-convex function with kernel  $\mathbf{v}$ , we have that

$$\nabla f(\mathbf{x})_j > 0 \Rightarrow j \in \text{argmax}_i (x_i - v_i).$$

**Theorem 26.** *Suppose  $f$  is a max-tropical location problem with respect to the dataset  $X = \{\mathbf{x}_1, \dots, \mathbf{x}_K\}$ . Let  $(\mathbf{t}_n)_{n \geq 1}$  be a sequence of points defined by tropical descent, such that for all  $n$ :  $\nabla f(\mathbf{t}_n) \neq \mathbf{0}$ . Let  $V = \text{tconv}_{\min}(\mathbf{x}_1, \dots, \mathbf{x}_K)$ , and define*

$$\Delta_i(\mathbf{t}) = \sum_{k \in [K]} \sum_{j \in [N]} [t_j - x_{kj} - t_i + x_{ki}]^+.$$

*For any  $\epsilon > 0$ , let  $M_1$  be such that for all  $m \geq M_1$ ,  $a_m \leq \epsilon/N$ . Let  $M_2$  be such that for all  $m \geq M_2$   $s_m \geq \max_i \Delta_i(\mathbf{t}_{M_1}) + s_{M_1} - K\epsilon$ . Then almost surely, for all  $m \geq M_2$  we have:*

$$d_{\text{tr}}(\mathbf{t}_m, V) \leq \epsilon.$$

*Proof.* For each  $i \leq N$ , we define the functions

$$\delta_i(\mathbf{t}) = \min_{k \in [K]} \left[ \sum_j [t_j - v_{kj} - t_i + v_{ki}]^+ \right].$$

**Claim 27.**  $d_{\text{tr}}(\mathbf{t}_m, V) \leq \max_j \delta_j(\mathbf{t}_m)$ .

*Proof.* As discussed in Maclagan & Sturmfels (2015), we have the projection map onto  $V$  given by:

$$\pi_V(\mathbf{t}) = \lambda_1 \odot \mathbf{x}_1 \oplus \cdots \oplus \lambda_K \odot \mathbf{x}_K, \quad \text{where } \lambda_k = \max_i (t_i - x_{ki})$$

So the distance to  $V$  is given by  $d(\mathbf{t}, \pi_V(\mathbf{t}))$ , and we have:

$$\begin{aligned} d(\mathbf{t}, V) &= d(\mathbf{t}, \pi_V(\mathbf{t})) \\ &= \|(\min_k (\max_i (t_i - x_{ki}) + x_{kj} - t_j))_j\| \\ &\leq \max_j (\min_k (\max_i (t_i - x_{ki}) + x_{kj} - t_j)) \\ &\leq \max_j \delta_j(\mathbf{t}) \end{aligned}$$

□

**Claim 28.** *If  $\delta_i(\mathbf{t}_m) = 0$  and  $m \geq M_1$ , then  $\delta_i(\mathbf{t}_{m+1}) < \epsilon$ .*

*Proof.* For all  $k \in [K], j \in [N]$ , we have that  $t_j - v_{kj} - t_i + v_{ki}$  is 1-Lipschitz in  $\mathbf{t}$ . Therefore  $\delta_i$  is  $N$ -Lipschitz in  $\mathbf{t}$ , and if  $\delta_i(\mathbf{t}_m) = 0$ ,  $\delta_i(\mathbf{t}_{m+1}) \leq Na_m < \epsilon$ . □

**Claim 29.** *If  $\delta_i(\mathbf{t}_m) > 0$  then  $\delta_i(\mathbf{t}_{m+1}) \leq \delta_i(\mathbf{t}_m)$ .*

*Proof.* Suppose  $\delta_i(\mathbf{t}_m) > 0$ . Then  $\forall k, \max_j (t_j - v_{kj}) > t_i - v_{ki}$ . By remark 25,  $\nabla f_i \leq 0$  and  $d_{mi} = 0$ . Therefore  $\delta_i(\mathbf{t}_{m+1}) \leq \delta_i(\mathbf{t}_m)$ . □

**Claim 30.** *Let  $M$  be such that  $s_M \geq \Delta_i(\mathbf{t}_{M_1}) + s_{M_1} - K\epsilon$ . Then for some  $M_1 \leq m \leq M$ ,  $\delta_i(\mathbf{t}_m) < \epsilon$ .*

*Proof.* We note that  $K\delta_i(\mathbf{t}) \leq \Delta_i(\mathbf{t})$ ; hence if  $\Delta_i(\mathbf{t}_{M_1}) < K\epsilon$  then we are done.

We now assume  $\Delta_i(\mathbf{t}_{M_1}) \geq K\epsilon$  and prove the result by contradiction; suppose  $\delta_i(\mathbf{t}_m) > \epsilon$  for all  $M_1 \leq m \leq M$ . Therefore at each step we have  $\nabla f_i \leq 0$ ,  $d_{mi} = 0$  and  $t_{mi}$  is fixed for  $n \leq M$ .

As  $\nabla f \neq \mathbf{0}$ , there is some  $j$  such that  $\nabla f_j > 0$ , and let  $k$  be such that  $j = \operatorname{argmax}_l t_{ml} - v_{kl}$ . As  $\delta_i(\mathbf{t}_m) > \epsilon$ :

$$t_j - v_{kj} - t_i + v_{ki} > \epsilon/N \geq a_m.$$

Hence this term in the summation of  $\Delta_i$  decreases by  $a_m$ , while other terms are non-increasing. We conclude that  $\Delta_i(\mathbf{t}_M) \leq \Delta_i(\mathbf{t}_{M_1}) - s_M + s_{M_1} \leq K\epsilon$ . Contradiction. □

Finally, from claims 28 to 30, we conclude that  $\forall m \geq M_2, i \leq N$ , we have  $\delta_i(\mathbf{t}_m) < \epsilon$ , and by claim 27, we have  $d_{\text{tr}}(\mathbf{t}_m, V) \leq \epsilon$ . □

As proven in Comăneci (2023), tropical location problems have minima in the tropical convex hull of the data. This result says that according to tropical gradient descent, only such minima can be stable. As a corollary, we can achieve the same result for min-tropical location problems by using negative tropical descent directions.

**Corollary 31.** *Suppose  $f$  is a min-tropical location problem with respect to the dataset  $X = \{\mathbf{x}_1, \dots, \mathbf{x}_K\}$ . Let  $(\mathbf{t}_n)_{n \geq 1}$  be a sequence of points defined via negative tropical descent directions, such that for all  $n$ :  $\nabla f(\mathbf{t}_n) \neq \mathbf{0}$ . Let  $V = \text{tconv}_{\max}(\mathbf{x}_1, \dots, \mathbf{x}_K)$ , and define*

$$\Delta'_j(\mathbf{t}) = \sum_{k \in [K]} \sum_{i \in [N]} [t_j - x_{kj} - t_i + x_{ki}]^+.$$

*For any initial  $\mathbf{t}_0$  and  $\epsilon > 0$ , let  $M_1$  be such that for all  $m \geq M_1$ ,  $a_m \leq \epsilon/N$ . Let  $M_2$  be such that for all  $m \geq M_2$   $s_m \geq \max_i \Delta'_j(\mathbf{t}_{M_1}) + s_{M_1} - K\epsilon$ . Then almost surely, for all  $m \geq M_2$  we have:*

$$d_{\text{tr}}(\mathbf{t}_n, V) \leq \epsilon.$$

Despite following from the previous results, the following corollary may be considered the most powerful result of this paper; tropical descent will necessarily minimise any max-tropically quasi-convex function.

**Corollary 32.** Let  $f(\mathbf{t})$  be a max-tropically quasiconvex function, and let  $(\mathbf{t}_n)_{n \geq 1}$  be a sequence of points defined by tropical descent such that for all  $n$ :  $\nabla f(\mathbf{t}_n) \neq 0$ . Then there is some global minimum  $\mathbf{t}^*$  such that for all  $m \leq M_2$ ,  $d_{\text{tr}}(\mathbf{t}_m, \mathbf{t}^*) \leq \epsilon$ .

We conclude by establishing the convergence rates of tropical descent in practice; we take step sizes given by  $a_m = \alpha m^{-1/2} \|\nabla f(\mathbf{t}_m)\|_{\text{tr}}$ , and assume gradients have bounded norm as in the case of piecewise linear objective functions. In this case, we prove convergence at a rate of  $O(\sqrt{m})$ .

**Proposition 33.** Suppose  $f$  is a max-tropical location problem as in Theorem 26. Assume that for all  $\mathbf{t}_m$ ,  $1/L \leq \|\nabla f(\mathbf{t}_m)\|_{\text{tr}} \leq 2$ , and assume further there is some  $D$  such that  $\forall k \leq K, n \in \mathbb{N}$ :  $d_{\text{tr}}(\mathbf{t}_n, \mathbf{x}_k) \leq D$ . We define  $a_m = \alpha m^{-1/2} \|\nabla f(\mathbf{t}_m)\|_{\text{tr}}$ . Then for all  $m$  satisfying

$$\sqrt{m+1}/2 - KDNL(N-1)/8\alpha + \sqrt{(\sqrt{m+1}/2 - KDNL(N-1)/8\alpha)^2 + LKN - 1} > \sqrt{2},$$

we have that:

$$d_{\text{tr}}(\mathbf{t}_m, V) \leq \frac{2\alpha N}{\sqrt{m+1} - KDNL(N-1)/4\alpha - 1} = \epsilon_m.$$

In particular, if  $f$  is max-tropically quasiconvex, then there is some global minimum  $\mathbf{t}^*$  such that

$$d_{\text{tr}}(\mathbf{t}_m, \mathbf{t}^*) \leq \frac{2\alpha N}{\sqrt{m+1} - DNL(N-1)/4\alpha - 1}.$$

*Proof.* We fix  $m$  and define:

$$M_1 = \left\lceil \left( \sqrt{m+1}/2 - KDNL(N-1)/8\alpha + \sqrt{(\sqrt{m+1}/2 - KDNL(N-1)/8\alpha)^2 + LKN - 1} \right)^2 \right\rceil.$$

We note that:

$$\begin{aligned} \sqrt{M_1} &\leq \sqrt{m+1}/2 - KDNL(N-1)/8\alpha + \sqrt{(\sqrt{m+1}/2 - KDNL(N-1)/8\alpha)^2 + LKN - 1}, \\ 0 \leq \sqrt{M_1} &\leq \frac{L}{2N} \left( \frac{N\sqrt{m+1}}{L} - \frac{KDN^2(N-1)}{4\alpha} + \sqrt{\left( \frac{N\sqrt{m+1}}{L} - \frac{KDN^2(N-1)}{4\alpha} \right)^2 + \frac{4N^2(LKN-1)}{L^2}} \right). \end{aligned}$$

So  $\sqrt{M_1}$  lies between the roots of the polynomial

$$p(t) = \frac{N}{L}t^2 + \left( \frac{KDN^2(N-1)}{4\alpha} - \frac{N\sqrt{m+1}}{L} \right)t + \frac{N - LKN^2}{L}.$$

Therefore:

$$\begin{aligned} 0 &\geq \frac{N}{L}M_1 + \left( \frac{KDN^2(N-1)}{4\alpha} - \frac{N\sqrt{m+1}}{L} \right) \sqrt{M_1} + \frac{N - LKN^2}{L} \\ \frac{N\sqrt{M_1}\sqrt{M_1+1}}{L} &\leq \left( \frac{N\sqrt{m+1}}{L} - \frac{KDN^2(N-1)}{4\alpha} \right) \sqrt{M_1} + KN^2 \\ KDN(N-1)/2 + 2\alpha L^{-1}(\sqrt{M_1+1} - \sqrt{m+1}) &\leq \frac{2\alpha KN}{\sqrt{M_1}} \end{aligned}$$

**Claim 34.** For all  $n \geq M_1$ , we have  $a_n \leq \epsilon_m/N$ .

*Proof.* We have assumed that

$$\sqrt{m+1}/2 - KDNL(N-1)/8\alpha + \sqrt{(\sqrt{m+1}/2 - KDNL(N-1)/8\alpha)^2 + LKN - 1} > \sqrt{2}$$

Then:

$$\begin{aligned}
M_1 &\geq \left( \sqrt{m+1}/2 - KDNL(N-1)/8\alpha + \sqrt{(\sqrt{m+1}/2 - KDNL(N-1)/8\alpha)^2 + LKN - 1} \right)^2 - 1 \\
&\geq \left( \sqrt{m+1}/2 - KDNL(N-1)/8\alpha + \sqrt{(\sqrt{m+1}/2 - KDNL(N-1)/8\alpha)^2 + LKN - 1 - 1} \right)^2 \\
\sqrt{M_1} &\geq \sqrt{m+1}/2 - KDNL(N-1)/8\alpha + \sqrt{(\sqrt{m+1}/2 - KDNL(N-1)/8\alpha)^2 + LKN - 1 - 1} \\
&\geq (\sqrt{m+1} - KDNL(N-1)/4\alpha) - 1
\end{aligned}$$

Hence:

$$\begin{aligned}
a_n &\leq \frac{2\alpha}{M_1^{1/2}} \\
&\leq \frac{2\alpha}{\sqrt{m+1} - KDNL(N-1)/4\alpha - 1} = \epsilon_m/N
\end{aligned}$$

□

**Claim 35.** For all  $n \geq m$ , we have  $\max_i \Delta_i(\mathbf{t}_{M_1}) + s_{M_1} - s_m \leq K\epsilon_m$ .

*Proof.* We note that

$$\begin{aligned}
\max_i \Delta_i(\mathbf{t}) &\leq \sum_i \Delta_i(\mathbf{t}) \\
&= \sum_{k \leq K} \sum_{i \leq j \leq N} |t_j - x_{kj} - t_i + x_{ki}| \\
&= \sum_{k \leq K} \sum_{i \leq j \leq N} d_{\text{tr}}(\mathbf{t}, \mathbf{x}_k),
\end{aligned}$$

and hence

$$\max_i \Delta_i(\mathbf{t}_{M_1}) \leq \frac{KDN(N-1)}{2}.$$

The partial sums are bounded by:

$$\begin{aligned}
s_{M_1} - s_m &\leq \sum_{n=M_1+1}^m -a_n \\
&\leq \sum_{n=M_1+1}^m \frac{-\alpha}{Ln^{1/2}} \\
&\leq -2\alpha L^{-1}(\sqrt{m+1} - \sqrt{M_1+1})
\end{aligned}$$

Therefore:

$$\begin{aligned}
\max_i \Delta_i(\mathbf{t}_{M_1}) + s_{M_1} - s_m &\leq KDN(N-1)/2 - 2\alpha L^{-1}(\sqrt{m+1} - \sqrt{M_1+1}) \\
&\leq \frac{2\alpha KN}{\sqrt{M_1}} \\
&\leq K\epsilon_m
\end{aligned}$$

□

Hence by Theorem 26, we have almost surely that

$$d_{\text{tr}}(\mathbf{t}_m, V) \leq \epsilon_m$$

The bound for the tropically quasiconvex case follows from Corollary 32.

□

## 4 Numerical Experiments

In this section we compare practical performance of classical descent, tropical descent, SGD, tropical SGD, Adam, Adamax, and Trop Adamax, with a focus on their stability behaviour. The implementation for all these experiments is available in an anonymous GitHub repository at <https://github.com/Roroast/TropicalGradDescent>.

### 4.1 Methods

**Descent** We will perform classical descent (CD) and tropical descent (TD) using equivalent same step size sequences  $a_n$  for both methods, which we fix as

$$a_n = \frac{\gamma \|\nabla f(\mathbf{t}_n)\|}{\sqrt{n}},$$

where  $\|\cdot\|$  is the Euclidean norm for classical descent and the tropical norm for tropical descent. When  $\nabla f(\mathbf{t})$  is bounded this is a well-behaved step rule;  $a_n$  will converge to 0. Furthermore, for the piecewise linear problems,  $\|\nabla f(\mathbf{t}_n)\|$  is bounded away from 0 almost everywhere which is not a global minimum. The convergence results of Section 3.2 will therefore apply.

**Stochastic Gradient Descent** Stochastic gradient descent is a variant of gradient descent which looks to improve computational speed by approximating  $\nabla f(t)$ ; rather than computing the loss and its gradient at  $\mathbf{t}$  with respect to the entire dataset  $f(\mathbf{t}; X)$ , we evaluate the loss and its gradient with respect to a random sample  $\mathbf{x}_n \in X$ ,  $f(\mathbf{t}; \mathbf{x}_n)$ . This is simplified with the notation  $f_n(\mathbf{t})$ . As with gradient descent, we use the step size sequence give by

$$a_n = \frac{\gamma \|\nabla f_n(\mathbf{t}_n)\|}{\sqrt{n}},$$

where  $\|\cdot\|$  is the Euclidean norm for stochastic gradient descent(SGD) and the tropical norm for tropical stochastic gradient descent (TropSGD).

**Adam Variants** The Adam algorithm (Kingma & Ba (2017)) uses gradient momentum to compound consistent but small effects. This is done by taking first and second moments of the gradient over all steps using exponentially decaying weights. The Adamax algorithm is a variant of the Adam algorithm motivated by the use of the  $\infty$ -moments rather than second moments.

To adapt the Adam algorithm for the tropical setting, we take moments of an un-normalized tropical descent direction. When looking to take higher moments of  $\mathbf{m}_n$  over  $n$ , the  $L_\infty$  is the natural option for the tropical setting. We therefore look to use the Adamax recursion relation on the  $\infty$ -moment estimate  $\mathbf{u}_n$ :

$$\mathbf{u}_{n+1} = \max(\beta_2 \mathbf{u}_n, \mathbf{d}_n).$$

We therefore define TropAdamax as in Algorithm 2.

---

#### Algorithm 2 TropAdamax

---

```

m, u  $\leftarrow$  0;
for  $n < \text{max\_steps}$  do
  g $_n$   $\leftarrow$   $\nabla f(\mathbf{t}_{n-1})$ ;
  d $_n$   $\leftarrow$   $[\mathbf{g}_n > 0] * (\max(\mathbf{g}_n) - \min(\mathbf{g}_n))$ ;
  m $_n$   $\leftarrow$   $\beta_1 * \mathbf{m}_{n-1} + (1 - \beta_1) * \mathbf{d}_n$ ;
  u $_n$   $\leftarrow$   $\max(\beta_2 * \mathbf{u}_{n-1}, |\mathbf{d}_n|)$ ;
  t $_n$   $\leftarrow$   $\mathbf{t}_n - \alpha / (1 - \beta_1^n) * \mathbf{m}_n / \mathbf{u}_n$ ;

```

---

## 4.2 Computation

We test the gradient methods discussed on 12 datasets of different sizes, shapes and dimensions; we consider datasets generated by a branching process, a coalescent process, or a Gaussian distribution on  $\mathbb{R}^N/\mathbb{R}\mathbf{1}$ , for  $N = 6, 28$  and samples of size 10 or 100. See Appendix A for further details on the simulated datasets. The learning rates used have been tuned for each gradient method and dataset size and dimension (Appendix C). In all experiments, random initialisations are taken from a Gaussian distribution on  $\mathbb{R}^N$ . We provide an overview of the general behaviour of each method for the various optimisation problems introduced in section 2.3.

Rather than investigating the relative convergence rates of each method, we are interested in the relative stability of local minima. We therefore plot the CDF of the relative log error after 1000 steps over 50 random initialisations, which can highlight certain error values at which several initialisations have accumulated. When the CDF of one method dominates another at log error =  $\epsilon$ , we expect it has a higher probability of achieving a log error of at most  $\epsilon$ .

### 4.2.1 Centrality Statistics

We first consider the behavior of tropical descent methods for the centrality statistics, Fermat–Weber points and Fréchet means. These optimisation problems are classically convex problems, as well as being both max-tropical and min-tropical location problems, and therefore lend themselves well to gradient methods. The experimental behaviour of these problems is similar, so in this section we include the results for the Fermat–Weber problem while the results for Fréchet means can be found in Appendix E.

Figure 5 shows the CDF of the final log relative error of the non-stochastic methods for the 12 datasets. We note that the stochastic methods achieves the worst error for all 12 datasets, and TropSGD is often performing worse than SGD. The disparity between SGD and TropSGD is greatest when the dimensionality of the data is greater than size of the dataset, while the disparity is smallest when the dimensionality is much smaller than the dataset size. We see similar behaviour in the log error of Tropical Descent and TropAdamax; they perform on par with their classical counterparts for each dataset other than the 28 by 10 datasets, but when the data dimensionality exceeds the number of data points, the tropical gradient methods are not achieving the same accuracy. We also note that convergence of all methods is less consistent for coalescent data than branching or Gaussian data; while it is unclear why this is, we note that coalescent data is supported on the space of ultrametric trees, which is a tropical hyperplane (Ardila & Klivans (2006); Page *et al.* (2020)) and may influence the uniqueness of minima.

Data	CD	TD	SGD	TropSGD	Adam	Adamax	TropAdamax
6×10 Branching Data	<b>-4.60</b>	<b>-4.60</b>	-4.48	-2.95	<b>-4.60</b>	<b>-4.60</b>	<b>-4.60</b>
6×10 Coalescent Data	<b>-4.58</b>	-4.55	-4.38	-1.34	<b>-4.58</b>	<b>-4.58</b>	-4.55
6×10 Gaussian Data	<b>-4.60</b>	<b>-4.60</b>	-4.44	-2.63	-4.58	-4.58	<b>-4.60</b>
6×100 Branching Data	<b>-4.60</b>	<b>-4.60</b>	-4.45	-3.95	-4.59	-4.59	-4.59
6×100 Coalescent Data	-4.55	-4.52	-4.37	-2.76	-4.54	<b>-4.57</b>	-4.54
6×100 Gaussian Data	<b>-4.60</b>	<b>-4.60</b>	-4.45	-4.00	-4.59	<b>-4.60</b>	-4.59
28×10 Branching Data	<b>-4.60</b>	<b>-4.60</b>	-4.15	-1.90	<b>-4.60</b>	<b>-4.60</b>	-4.56
28×10 Coalescent Data	-4.52	-3.76	-3.99	-2.24	-4.52	<b>-4.56</b>	-3.84
28×10 Gaussian Data	-4.59	-4.59	-4.09	-2.47	<b>-4.60</b>	<b>-4.60</b>	-4.47
28×100 Branching Data	<b>-4.59</b>	<b>-4.59</b>	-4.05	-3.13	<b>-4.59</b>	<b>-4.59</b>	<b>-4.59</b>
28×100 Coalescent Data	-4.49	-4.47	-3.86	-2.54	-4.38	<b>-4.56</b>	-4.48
28×100 Gaussian Data	<b>-4.59</b>	<b>-4.59</b>	-4.09	-3.02	<b>-4.59</b>	<b>-4.59</b>	-4.56

Table 1: The mean log relative error of each gradient method after 1000 steps for each dataset when minimising the Fermat–Weber objective function. The minimal mean errors for each dataset are in bold.

### 4.2.2 Wasserstein Projections

The Wasserstein projection problems highlight the differences in convergent behaviour with and without the tropical gradient, as they are max-tropical location problems, but not classically convex. The CDFs of the

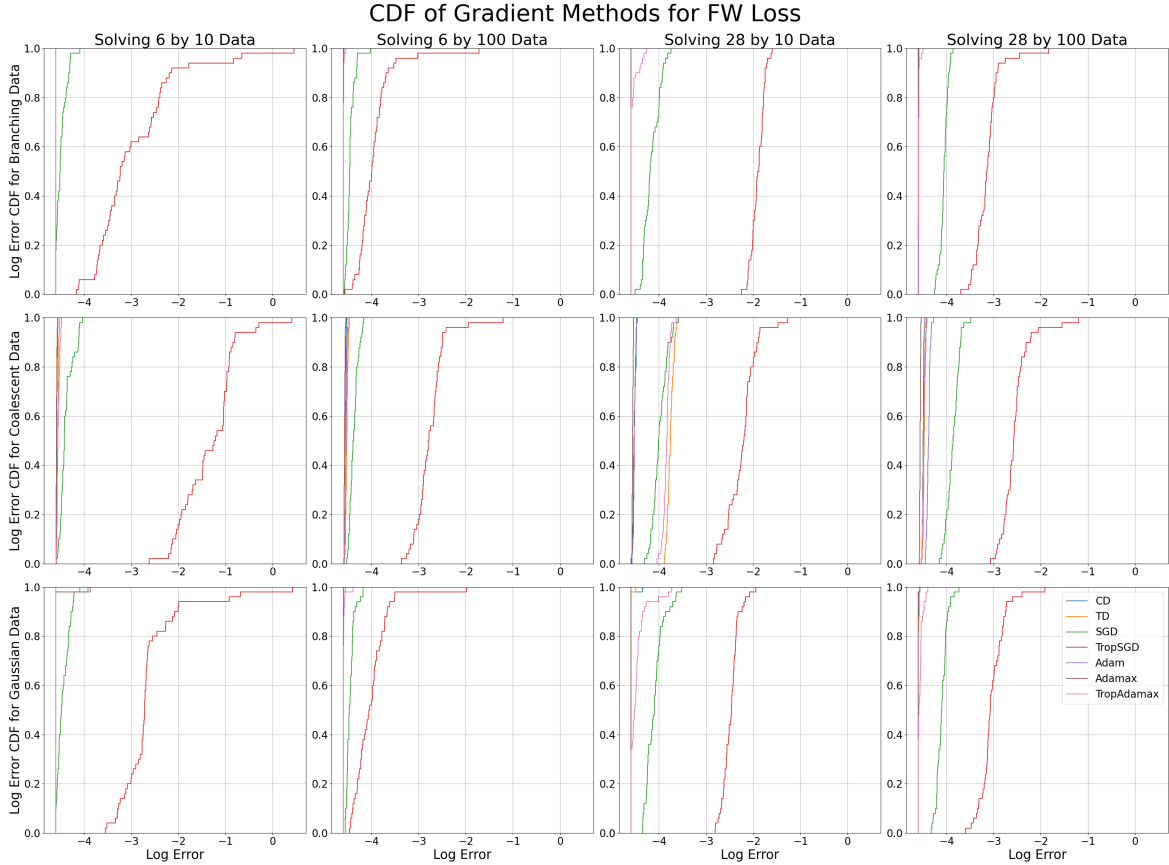


Figure 5: The CDF of the log relative error after 1000 steps for each gradient method across 50 initialisations when minimising the Fermat–Weber objective. Each subfigure corresponds to a dataset of different dimensionality (columns) and distribution (rows).

final log relative errors can be found in Figures 6 and 7.

In Figures 6 and 7 we see large steps at various intervals in the CDF plots, which is indicative of stable local minima. This is particularly prevalent in low dimensional space. Classical descent, Adam, and Adamax are particularly susceptible to this, while tropical descent and TropAdamax are often more likely to pass these local minima. This difference is most pronounced when solving the  $\infty$ -Wasserstein problem in low dimensions—we are almost certain to reach the minimum with small error, while classical methods have a 50-80% chance of achieving the same error.

From tables 2 and 3, we see that when solving the 2-Wasserstein projection problem, tropical methods are optimal in all cases other than  $28 \times 10$  coalescent data. For the  $\infty$ -Wasserstein projection problem in small dimensions, tropical descent outperforms other methods by some margin, while the comparative performances are less consistent for the  $\infty$ -Wasserstein projection problem in high dimensions.

### 4.2.3 Linear Regression

The linear regression problem is a min tropical location problem, so we run the same code with input  $-\mathbf{t}$ . As the coalescent data lies on a tropical hyperplane (Ardila & Klivans (2006); Page *et al.* (2020)), the minimum of the linear regression function for such data is exactly 0. Figure 8 therefore shows the CDF of the log error rather than the CDF of the log relative error.

As we can see in table 4, the tropical methods outperform their classical counterparts for every dataset, often by a factor of two. The tropical descent method in particular is the most effective for all but one dataset. In Figure 8 we see that the CDF of log errors for tropical descent and TropAdamax consistently

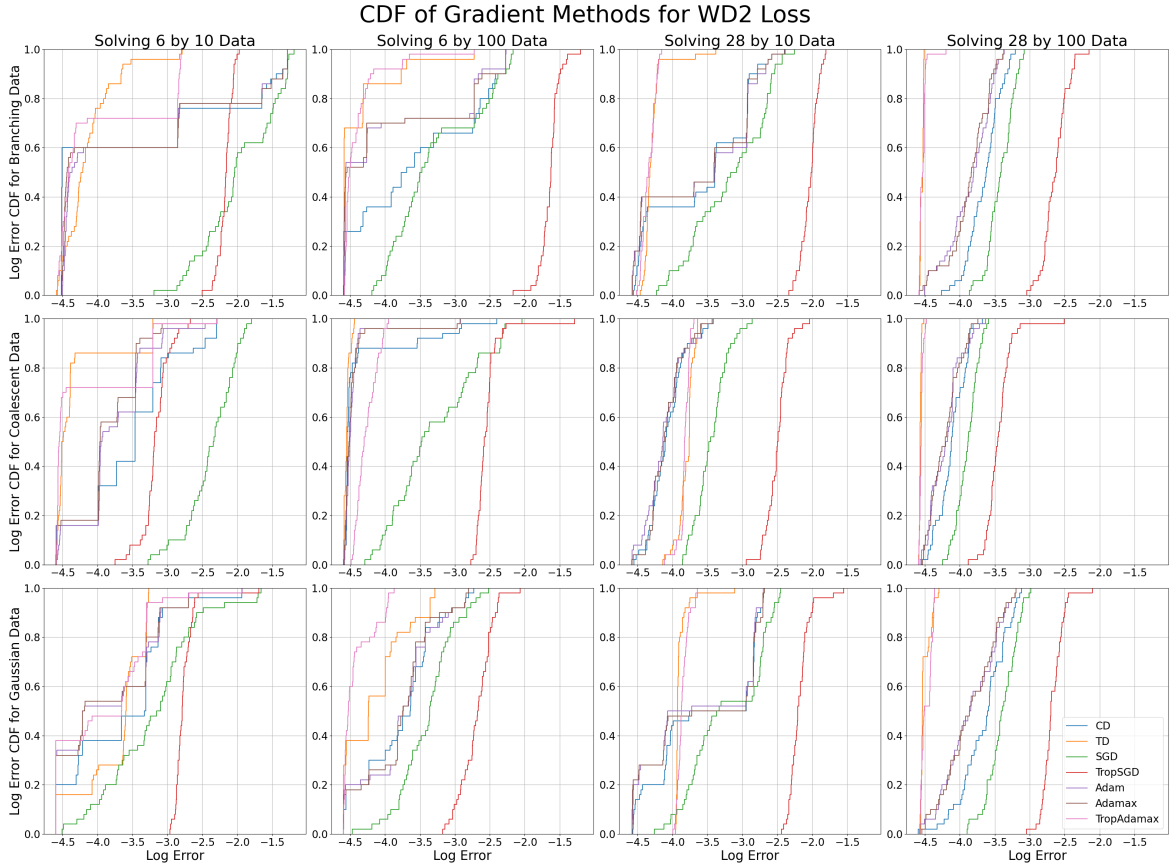


Figure 6: The CDF of the log relative error after 1000 steps for each gradient method across 50 initialisations when minimising the 2-Wasserstein projection objective. Each subfigure corresponds to a dataset of different dimensionality (columns) and distribution (rows).

Data	CD	TD	SGD	TropSGD	Adam	Adamax	TropAdamax
6×10 Branching Data	-3.52	<b>-4.13</b>	-1.98	-2.17	-3.49	-3.51	-3.99
6×10 Coalescent Data	-3.53	<b>-4.31</b>	-2.38	-3.17	-3.77	-3.85	-4.16
6×10 Gaussian Data	-3.66	-3.72	-3.21	-2.76	-3.84	-3.85	<b>-3.90</b>
6×100 Branching Data	-3.57	-4.38	-3.28	-1.64	-3.94	-3.94	<b>-4.39</b>
6×100 Coalescent Data	-4.35	<b>-4.54</b>	-3.31	-2.54	-4.43	-4.44	-4.26
6×100 Gaussian Data	-3.78	-4.15	-3.39	-2.69	-3.77	-3.79	<b>-4.42</b>
28×10 Branching Data	-3.59	-4.29	-3.18	-2.03	-3.63	-3.64	<b>-4.34</b>
28×10 Coalescent Data	-4.07	-3.80	-3.45	-2.50	<b>-4.12</b>	-4.09	-3.82
28×10 Gaussian Data	-3.53	<b>-3.89</b>	-3.22	-2.18	-3.61	-3.58	-3.85
28×100 Branching Data	-3.65	<b>-4.54</b>	-3.42	-2.64	-3.86	-3.87	-4.53
28×100 Coalescent Data	-4.12	<b>-4.57</b>	-3.89	-3.44	-4.20	-4.21	-4.55
28×100 Gaussian Data	-3.65	<b>-4.50</b>	-3.39	-2.67	-3.85	-3.86	-4.48

Table 2: The mean log relative error of each gradient method after 1000 steps for each dataset when minimising the 2-Wasserstein projection objective function. The minimal mean errors for each dataset are in bold.



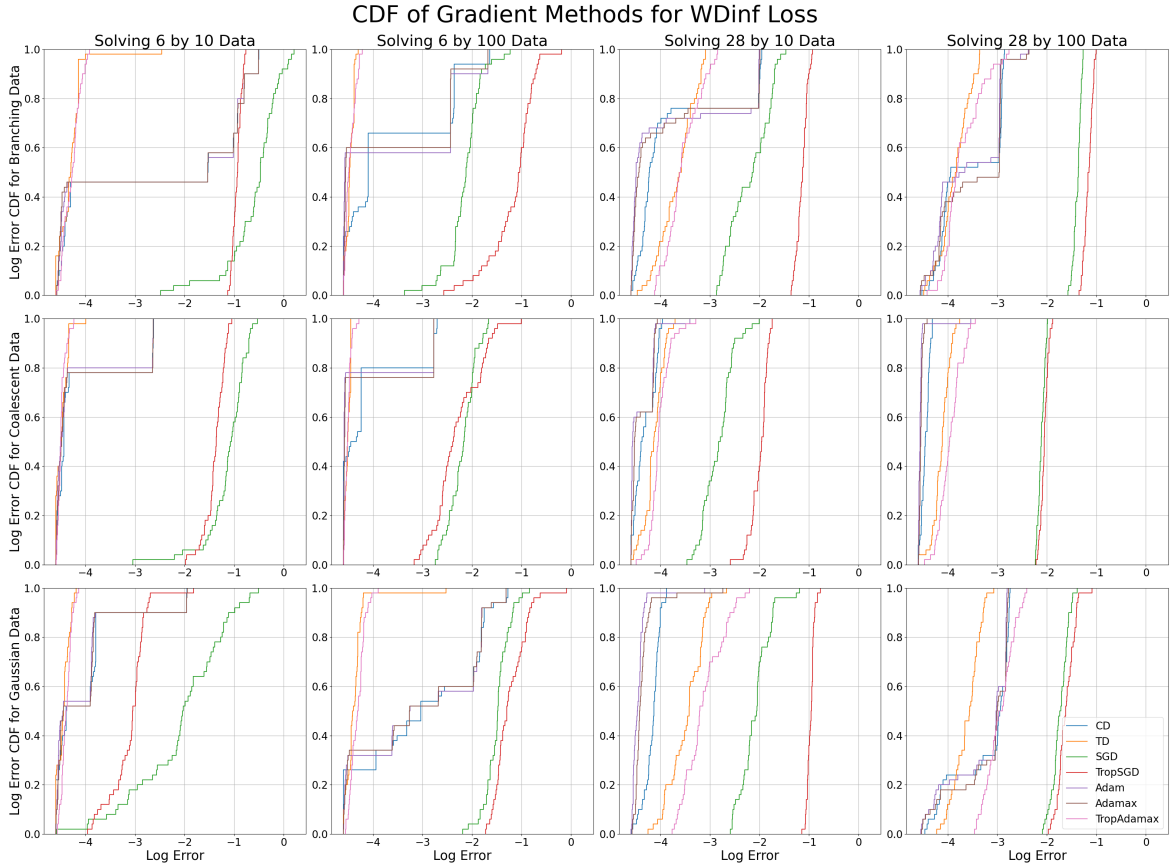


Figure 7: The CDF of the log relative error after 1000 steps for each gradient method across 50 initialisations when minimising the  $\infty$ -Wasserstein projection objective. Each subfigure corresponds to a dataset of different dimensionality (columns) and distribution (rows).

Data	CD	TD	SGD	TropSGD	Adam	Adamax	TropAdamax
6×10 Branching Data	-2.56	<b>-4.29</b>	-0.58	-0.94	-2.58	-2.59	-4.28
6×10 Coalescent Data	-4.07	<b>-4.48</b>	-1.13	-1.38	-4.13	-4.09	<b>-4.48</b>
6×10 Gaussian Data	-4.00	<b>-4.44</b>	-2.08	-3.10	-4.04	-4.02	-4.38
6×100 Branching Data	-3.63	<b>-4.46</b>	-2.14	-1.17	-3.60	-3.65	<b>-4.46</b>
6×100 Coalescent Data	-4.11	<b>-4.51</b>	-2.19	-2.30	-4.18	-4.14	<b>-4.51</b>
6×100 Gaussian Data	-3.02	<b>-4.36</b>	-1.48	-1.23	-3.06	-3.09	-4.31
28×10 Branching Data	-3.72	-3.66	-2.19	-1.14	<b>-3.81</b>	<b>-3.81</b>	-3.55
28×10 Coalescent Data	-4.31	-4.13	-2.83	-1.99	<b>-4.39</b>	<b>-4.39</b>	-4.01
28×10 Gaussian Data	-4.16	-3.47	-2.08	-0.96	<b>-4.43</b>	-4.36	-3.12
28×100 Branching Data	-3.55	<b>-3.86</b>	-1.38	-1.16	-3.59	-3.49	-3.71
28×100 Coalescent Data	-4.45	-4.12	-2.11	-2.05	<b>-4.54</b>	<b>-4.54</b>	-3.95
28×100 Gaussian Data	-3.23	<b>-3.61</b>	-1.74	-1.61	-3.27	-3.22	-2.94

Table 3: The mean log relative error of each gradient method after 1000 steps for each dataset when minimising the  $\infty$ -Wasserstein projection objective function. The minimal mean errors for each dataset are in bold.

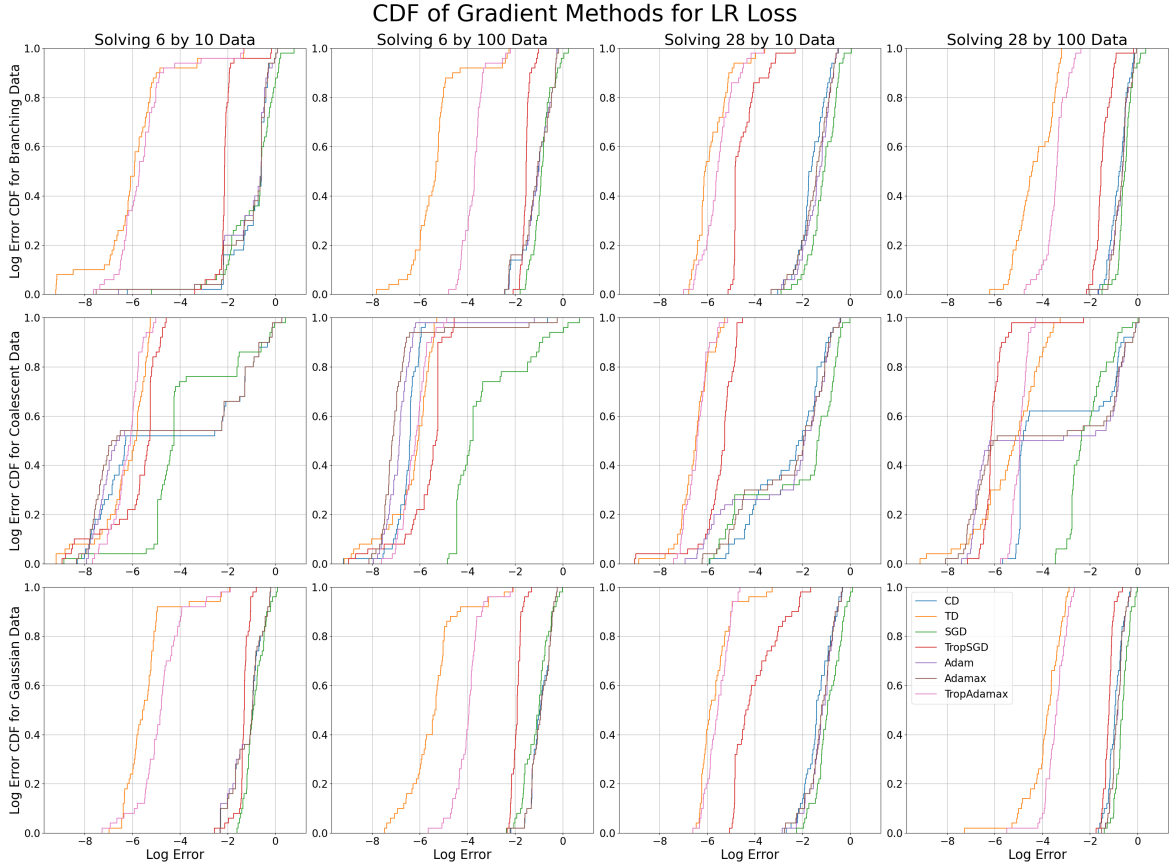


Figure 8: The CDF of the log relative error after 1000 steps for each gradient method across 50 initialisations when minimising the linear regression objective. Each subfigure corresponds to a dataset of different dimensionality (columns) and distribution (rows).

dominates those of classical descent, Adam and Adamax, to the extent that the support of their CDFs does not intersect that of their classical counterparts for some datasets. We also note that unlike the previous problems, TropSGD is outperforming SGD when solving the linear regression problem, often to the extent that TropSGD outperforms all classical gradient methods.

## 5 Discussion

We have introduced the concept of tropical descent as the steepest descent method with respect to the tropical norm. We have demonstrated, both theoretically and experimentally, that it possesses well-behaved properties with respect to a wide class of optimisation problems on the tropical projective torus, including several key statistical problems for the analysis of phylogenetic data. However, our experimental results are stronger than our theoretical results suggest; the optimisation problems studied are location problems, rather than  $\Delta$ -star-quasi-convex problems, and yet tropical descent appears to consistently converge to a global minimum, not just the tropical convex hull of our dataset. It would therefore be a natural extension of this work to identify how much we can relax the  $\Delta$ -star-quasi-convexity condition while guaranteeing convergence.

In this paper, we consider tree data with 4 to 8 leaves, and samples of size 10 to 100—at this scale, we have observed (Trop/)SGD to be a significant sacrifice in accuracy with little benefit in computational time. Furthermore, at this scale, the relative merits of SGD versus its tropical counterpart are inconsistent; TropSGD out-performs SGD when solving the linear regression problem, but performs worse when finding

Data	CD	TD	SGD	TropSGD	Adam	Adamax	TropAdamax
6×10 Branching Data	-0.96	<b>-5.96</b>	-0.92	-2.10	-1.09	-1.07	-5.57
6×10 Coalescent Data	-4.27	<b>-6.25</b>	-3.80	-5.78	-4.44	-4.54	-6.22
6×10 Gaussian Data	-1.13	<b>-5.42</b>	-0.86	-1.33	-1.15	-1.14	-4.79
6×100 Branching Data	-1.08	<b>-5.34</b>	-0.86	-1.54	-1.10	-1.11	-3.73
6×100 Coalescent Data	-6.42	-6.35	-3.29	-5.69	-6.81	<b>-6.88</b>	-6.22
6×100 Gaussian Data	-0.93	<b>-5.43</b>	-1.09	-1.93	-0.92	-0.92	-3.97
28×10 Branching Data	-1.60	<b>-5.83</b>	-1.13	-4.47	-1.41	-1.48	-5.53
28×10 Coalescent Data	-2.56	<b>-6.52</b>	-2.22	-5.50	-2.68	-2.61	-6.44
28×10 Gaussian Data	-1.35	<b>-5.68</b>	-0.91	-3.99	-1.20	-1.23	-5.56
28×100 Branching Data	-0.79	<b>-4.33</b>	-0.54	-1.46	-0.69	-0.70	-3.44
28×100 Coalescent Data	-3.35	<b>-5.34</b>	-2.10	-6.04	-3.79	-3.94	-4.95
28×100 Gaussian Data	-0.93	<b>-3.88</b>	-0.64	-1.22	-0.84	-0.85	-3.44

Table 4: The mean log relative error of each gradient method after 1000 steps for each dataset when minimising the linear regression objective function. The minimal mean errors for each dataset are in bold.

centrality statistics. However, for applications to larger datasets, we would expect the stochastic approaches to be more suitable. It would then be important to understand the theoretical differences between SGD and TropSGD in terms of their convergence guarantees in the tropical setting and their comparative performance in practice.

Finally, as shown by Akian *et al.* (2023), the tropical linear regression problem is polynomial-time equivalent to mean payoff games - two-player perfect information games on a directed graph (Ehrenfeucht & Mycielski (1979); Gurvich *et al.* (1988)). This family of problems of particular interest in game theory as they are known to be  $NP \cap co-NP$ . While our methods are designed to approximate the minimum rather than compute it exactly, tropical descent may prove to be an efficient tool when solving large-scale mean payoff games.

## Acknowledgments

R.T. receives partial funding from a Technical University of Munich-Imperial College London Joint Academy of Doctoral Studies (JADS) award (2021 cohort, PIs Drton/Monod). A.M. is supported by the Engineering and Physical Sciences Research Council under grant reference [EP/Y028872/1] and a London Mathematical Society Emmy Noether Fellowship.

## References

- AKIAN, MARIANNE, GAUBERT, STÉPHANE, QI, YANG, & SAADI, OMAR. 2023. Tropical Linear Regression and Mean Payoff Games: Or, How to Measure the Distance to Equilibria. *SIAM Journal on Discrete Mathematics*, **37**(2), 632–674.
- ALIATIMIS, GEORGIOS, YOSHIDA, RURIKO, BOYACI, BURAK, & GRANT, JAMES A. 2023. Tropical Logistic Regression Model on Space of Phylogenetic Trees. *arXiv preprint arXiv:2306.08796*.
- ARDILA, FEDERICO, & KLIVANS, CAROLINE J. 2006. The Bergman complex of a matroid and phylogenetic trees. *Journal of Combinatorial Theory, Series B*, **96**(1), 38–49.
- BOYD, STEPHEN P, & VANDENBERGHE, LIEVEN. 2004. *Convex optimization*. Cambridge university press.
- CAI, YUHANG, & LIM, LEK-HENG. 2022. Distances Between Probability Distributions of Different Dimensions. *IEEE Transactions on Information Theory*, **68**(6), 4020–4031.
- COMĂNECI, ANDREI. 2023. Tropical convexity in location problems. *arXiv preprint arXiv:2307.04465*.

- COMĂNECI, ANDREI, & JOSWIG, MICHAEL. 2023. Tropical medians by transportation. *Mathematical Programming*, 1–27.
- DEVELIN, MIKE, & STURMFELS, BERND. 2004. Tropical convexity. *Documenta Mathematica*, **9**, 1–27.
- EHRENFEUCHT, ANDRZEJ, & MYCIELSKI, JAN. 1979. Positional strategies for mean payoff games. *International Journal of Game Theory*, **8**, 109–113.
- FRÉCHET, MAURICE. 1948. Les éléments aléatoires de nature quelconque dans un espace distancié. *Pages 215–310 of: Annales de l'institut Henri Poincaré*, vol. 10.
- GURVICH, VA, KARZANOV, AV, & KHACHIYAN, LG. 1988. Cyclic games and finding minimax mean cycles in digraphs. *Zh. Vychisl. Mat. i Mat. Fiz.*, **28**(9), 1407–1417.
- HARRIS, CHARLES R., MILLMAN, K. JARROD, VAN DER WALT, STÉFAN J., GOMMERS, RALF, VIRTANEN, PAULI, COURNAPEAU, DAVID, WIESER, ERIC, TAYLOR, JULIAN, BERG, SEBASTIAN, SMITH, NATHANIEL J., KERN, ROBERT, PICUS, MATTI, HOYER, STEPHAN, VAN KERKWIJK, MARTEN H., BRETT, MATTHEW, HALDANE, ALLAN, DEL RÍO, JAIME FERNÁNDEZ, WIEBE, MARK, PETERSON, PEARU, GÉRARD-MARCHANT, PIERRE, SHEPPARD, KEVIN, REDDY, TYLER, WECKESSER, WARREN, ABBASI, HAMEER, GOHLKE, CHRISTOPH, & OLIPHANT, TRAVIS E. 2020. Array programming with NumPy. *Nature*, **585**(7825), 357–362.
- JAZLAN, ARIFF, MONOD, ANTHEA, & MATTEO, BEATRICE. 2024+. *Tropical Fréchet Means*.
- KINGMA, DIEDERIK P., & BA, JIMMY. 2017. *Adam: A Method for Stochastic Optimization*.
- KIWIEL, KRZYSZTOF C. 2006. *Methods of descent for nondifferentiable optimization*. Vol. 1133. Springer.
- LAPORTE, GILBERT, NICKEL, STEFAN, & SALDANHA-DA GAMA, FRANCISCO. 2019. *Introduction to location science*. Springer.
- LEE, WONJUN, LI, WUCHEN, LIN, BO, & MONOD, ANTHEA. 2021. Tropical optimal transport and Wasserstein distances. *Information Geometry*, 1–41.
- LIN, BO, & TRAN, NGOC MAI. 2019. Two-player incentive compatible outcome functions are affine maximizers. *Linear Algebra and its Applications*, **578**, 133–152.
- LIN, BO, & YOSHIDA, RURIKO. 2018. Tropical Fermat–Weber Points. *SIAM Journal on Discrete Mathematics*, **32**(2), 1229–1245.
- MACLAGAN, DIANE, & STURMFELS, BERND. 2015. *Introduction to tropical geometry*. Vol. 161. American Mathematical Soc.
- MACLAGAN, DIANE, & STURMFELS, BERND. 2021. *Introduction to tropical geometry*. Vol. 161. American Mathematical Society.
- MONOD, ANTHEA, LIN, BO, YOSHIDA, RURIKO, & KANG, QIWEN. 2018. Tropical geometry of phylogenetic tree space: a statistical perspective. *arXiv preprint arXiv:1805.12400*.
- MONOD, ANTHEA, LIN, BO, YOSHIDA, RURIKO, & KANG, QIWEN. 2022. *Tropical Geometry of Phylogenetic Tree Space: A Statistical Perspective*.
- PAGE, ROBERT, YOSHIDA, RURIKO, & ZHANG, LEON. 2020. Tropical principal component analysis on the space of phylogenetic trees. *Bioinformatics*, **36**(17), 4590–4598.
- PARADIS, EMMANUEL, & SCHLIEP, KLAUS. 2019. ape 5.0: an environment for modern phylogenetics and evolutionary analyses in R. *Bioinformatics*, **35**(3), 526–528.
- SPEYER, DAVID, & STURMFELS, BERND. 2004. The Tropical Grassmannian. *Adv. Geom.*, **4**(3), 389–411.
- TALBUT, ROAN, TRAMONTANO, DANIELE, CAO, YUEQI, DRTON, MATHIAS, & MONOD, ANTHEA. 2023. *Probability Metrics for Tropical Spaces of Different Dimensions*.

WESOŁOWSKY, GEORGE O. 1993. The Weber Problem: History and Perspectives. *Computers & Operations Research*.

YOSHIDA, RURIKO. 2020. *Tropical Data Science*.

YOSHIDA, RURIKO, ZHANG, LEON, & ZHANG, XU. 2019. Tropical principal component analysis and its application to phylogenetics. *Bulletin of mathematical biology*, **81**(2), 568–597.

# A Data Generation

The same 12 datasets are used for each experiment in Section 4. These datasets live in  $\mathbb{R}^6/\mathbb{R}\mathbf{1}$  or  $\mathbb{R}^{28}/\mathbb{R}\mathbf{1}$ ; these dimensions correspond to the spaces of trees with 4 and 8 leaves respectively. Branching process datasets are generated using the R package `ape` (Paradis & Schliep (2019)) with exponentially distributed branch lengths—this produces data supported on the space of metric trees, i.e., the tropical Grassmannian. Coalescent data has also been generated using `ape` and is supported on the space of ultrametric trees, which is a tropical linear space. Gaussian data is generated using NumPy (Harris *et al.* (2020)), and is supported on the general tropical projective torus.

In the computation of the Wasserstein projection objectives, we require a secondary dataset of different dimensionality; for each of the 12 datasets, we generate datasets of the same size and distribution, but in  $\mathbb{R}^3/\mathbb{R}\mathbf{1}$  or  $\mathbb{R}^{21}/\mathbb{R}\mathbf{1}$  which contain the spaces of trees with 3 and 7 leaves respectively.

# B PCA and Logistic Regression

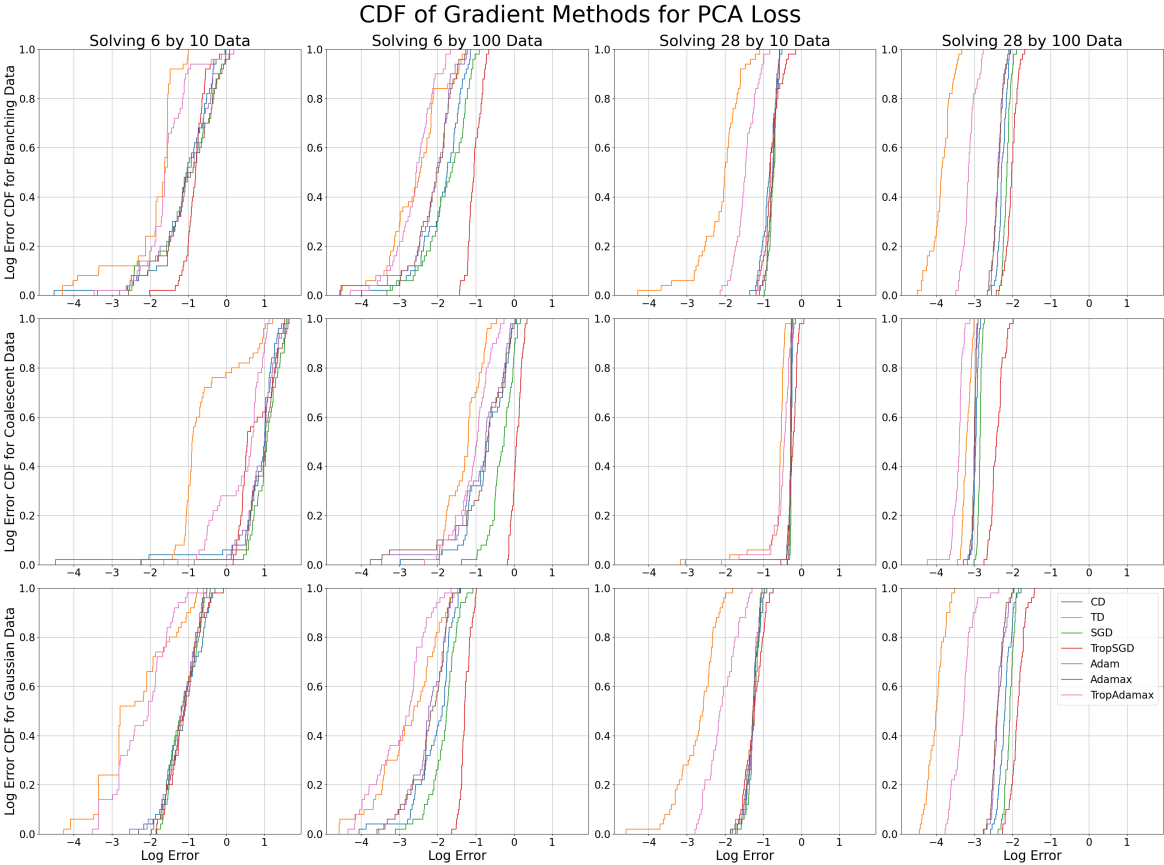


Figure 9: The CDF of the log relative error after 1000 steps for each gradient method across 50 initialisations when minimising the PCA objective. Each subfigure corresponds to a dataset of different dimensionality (columns) and distribution (rows).

As well as the location problems outlined in this paper, we performed the same numerical experiments with the tropical polytope PCA loss function (Yoshida *et al.* (2019)) and tropical logistic regression loss function (Aliatimis *et al.* (2023)). These loss functions take multiple points in  $\mathbb{R}^N/\mathbb{R}\mathbf{1}$  as argument, and we execute our gradient methods on each argument simultaneously. Figures 9 and 10 show the resulting CDF of our gradient methods for these problems. These problems do not lend themselves well to gradient methods,

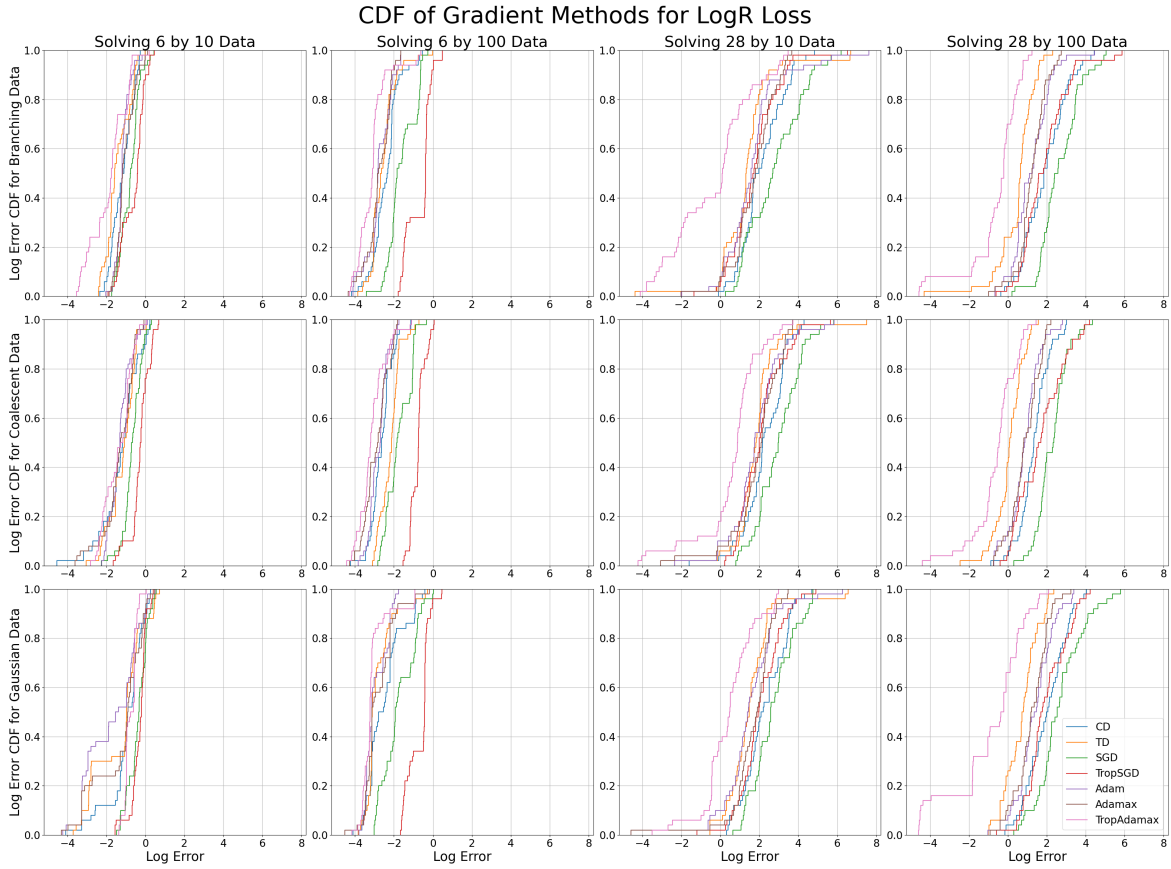


Figure 10: The CDF of the log relative error after 1000 steps for each gradient method across 50 initialisations when minimising the logistic regression objective. Each subfigure corresponds to a dataset of different dimensionality (columns) and distribution (rows).

as the relative log error is rather large for all of our proposed methods. However, for both problems the tropical descent and TropAdamax methods are outperforming the classical methods quite consistently.

## C Learning Rate Tuning

The Adam algorithms—Adam, Adamax and TropAdamax—are run using the default  $\beta = (0.9, 0.999)$  parameters. We then tune the learning rates used for each method; Gradient Descent, Tropical Descent, SGD, Tropical SGD, Adam, Adamax, and TropAdamax. We perform an initial test of learning rates  $\gamma = 0.0001, 0.0003, 0.001, 0.003, 0.01, 0.03, 0.1, 0.3, 1, 3, 10, 30$  over 1000 steps for each algorithm, with 5 random initialisations for each dataset. From this, we narrowed our search to take 18 initializations at 0.5 intervals on the log scale in near optimal regions for each problem, gradient method, and data dimensionality. We then selected the learning rate with minimal mean log relative error in each case; tables 5 - 11 show the selected learning rates.

Data Dim	Data Count	CD	TD	SGD	TropSGD	Adam	Adamax	TropAdamax
6	10	0.135	0.135	0.135	0.0821	0.00409	0.00409	0.0111
	100	0.135	0.135	0.0821	0.135	0.00409	0.00409	0.00674
28	10	0.368	0.368	0.368	0.607	0.00674	0.00674	0.0183
	100	0.368	0.223	0.368	0.607	0.00674	0.00674	0.0111

Table 5: Learning rates for each gradient method when solving the Fermat–Weber problem.

Data Dim	Data Count	CD	TD	SGD	TropSGD	Adam	Adamax	TropAdamax
6	10	0.135	0.135	0.135	0.135	0.00674	0.00674	0.00674
	100	0.135	0.0821	0.0821	0.223	0.00674	0.00674	0.0111
28	10	0.368	0.223	0.223	0.607	0.00674	0.00674	0.0183
	100	0.368	0.135	0.223	0.607	0.00674	0.00674	0.0111

Table 6: Learning rates for each gradient method when solving the Fréchet mean problem.

Data Dim	Data Count	CD	TD	SGD	TropSGD	Adam	Adamax	TropAdamax
6	10	1.65	7.39	0.0821	0.223	0.135	0.223	0.0821
	100	1.65	4.48	0.368	0.135	0.0821	0.135	1.00
28	10	1.65	0.368	0.607	0.607	0.00674	0.0111	0.0183
	100	2.72	2.72	0.368	0.607	0.0302	0.0821	0.0498

Table 7: Learning rates for each gradient method when solving the 2-Wasserstein projection problem.

Data Dim	Data Count	CD	TD	SGD	TropSGD	Adam	Adamax	TropAdamax
6	10	0.0821	0.135	0.0302	0.223	0.00674	0.00674	0.0183
	100	0.368	0.135	0.607	0.0498	0.00248	0.00409	0.0183
28	10	0.223	0.607	0.223	0.607	0.00409	0.0111	0.0821
	100	0.223	0.607	0.223	0.607	0.00409	0.0111	0.0821

Table 8: Learning rates for each gradient method when solving the  $\infty$ -Wasserstein projection problem.

Data Dim	Data Count	CD	TD	SGD	TropSGD	Adam	Adamax	TropAdamax
6	10	2.72	4.48	0.607	1.65	0.135	0.135	0.368
	100	2.72	4.48	1.00	0.607	0.0821	0.135	0.607
28	10	7.39	4.48	0.368	1.65	0.0183	0.0183	0.223
	100	4.48	7.39	0.368	0.607	0.0302	0.0821	0.0821

Table 9: Learning rates for each gradient method when solving the polytope PCA problem.



Data Dim	Data Count	CD	TD	SGD	TropSGD	Adam	Adamax	TropAdamax
6	10	7.39	12.2	1.00	2.72	1.00	1.00	0.607
	100	7.39	12.2	1.00	0.368	0.607	1.00	1.00
28	10	20.1	245	7.39	90.0	4.48	4.48	2.72
	100	20.1	90.0	4.48	90.0	1.65	7.39	2.72

Table 10: Learning rates for each gradient method when solving the logistic regression problem.

Data Dim	Data Count	CD	TD	SGD	TropSGD	Adam	Adamax	TropAdamax
6	10	0.0302	0.0821	0.223	0.0821	0.00248	0.00248	0.0111
	100	0.0498	0.0821	0.368	0.0821	0.00248	0.00248	0.0111
28	10	0.368	0.0821	0.0821	0.135	0.0111	0.0302	0.0111
	100	0.223	0.607	1.00	12.2	0.0015	0.00409	0.0498

Table 11: Learning rates for each gradient method when solving the linear regression problem.

## D Runtimes

Experiments were implemented on a AMD EPYC 7742 node using a single core, 8 GB. Table 12 shows the average time taken per initialisation for each gradient method and optimisation problem.

Stats Prob	CD	TD	SGD	TropSGD	Adam	Adamax	TropAdamax
Fermat–Weber	0.18s	0.19s	0.26s	0.26s	0.22s	0.23s	0.26s
Fréchet Mean	0.23s	0.23s	0.30s	0.30s	0.28s	0.28s	0.31s
2-Wasserstein Projection	1.18s	1.18s	1.75s	1.77s	1.23s	1.24s	1.27s
$\infty$ -Wasserstein Projection	1.17s	1.17s	1.71s	1.71s	1.21s	1.21s	1.24s
Polytope PCA	0.60s	0.61s	0.78s	0.78s	0.64s	0.64s	0.68s
Logistic Regression	0.45s	0.45s	0.62s	0.62s	0.68s	0.50s	0.53s
Linear Regression	0.22s	0.22s	0.27s	0.28s	0.26s	0.27s	0.30s

Table 12: Average runtimes for 1000 steps of each gradient method when minimising each objective function.

## E Further Figures

Here we include the results for experiments run for the computation of Fréchet means.

Data	CD	TD	SGD	TropSGD	Adam	Adamax	TropAdamax
6×10 Branching Data	<b>-4.59</b>	-4.56	-4.01	-2.93	-4.58	<b>-4.59</b>	-4.54
6×10 Coalescent Data	<b>-4.58</b>	-4.49	-4.06	-1.86	-4.57	<b>-4.58</b>	-4.50
6×10 Gaussian Data	<b>-4.59</b>	-4.35	-4.10	-2.63	-4.58	<b>-4.59</b>	-4.32
6×100 Branching Data	<b>-4.60</b>	-4.59	-4.36	-3.90	-4.59	-4.59	-4.59
6×100 Coalescent Data	<b>-4.57</b>	<b>-4.57</b>	-4.44	-3.14	-4.54	-4.56	-4.55
6×100 Gaussian Data	-4.59	-4.59	-4.44	-4.03	-4.59	<b>-4.60</b>	-4.59
28×10 Branching Data	<b>-4.57</b>	-3.69	-3.66	-1.99	-4.54	<b>-4.57</b>	-3.79
28×10 Coalescent Data	-4.56	-3.72	-4.01	-2.57	-4.52	<b>-4.57</b>	-3.71
28×10 Gaussian Data	-4.56	-4.05	-3.71	-2.49	-4.54	<b>-4.57</b>	-4.02
28×100 Branching Data	<b>-4.59</b>	-4.58	-3.99	-3.23	-4.58	<b>-4.59</b>	-4.58
28×100 Coalescent Data	-4.54	-4.56	-4.14	-2.87	-4.46	<b>-4.57</b>	-4.52
28×100 Gaussian Data	<b>-4.59</b>	-4.55	-3.90	-3.01	<b>-4.59</b>	<b>-4.59</b>	-4.58

Table 13: The mean log relative error of each gradient method after 1000 steps for each dataset when minimising the Fréchet mean objective function. The minimal mean errors for each dataset are in bold.

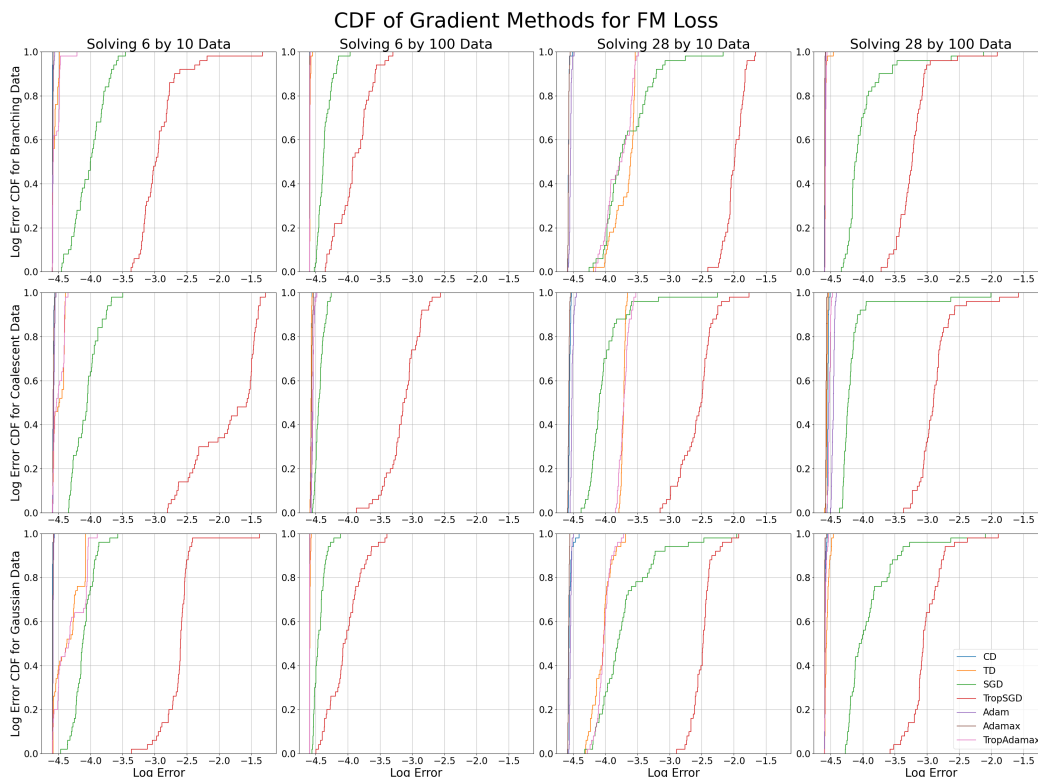


Figure 11: The CDF of the log relative error after 1000 steps for each gradient method across 50 initialisations when minimising the Fréchet mean objective. Each subfigure corresponds to a dataset of different dimensionality (columns) and distribution (rows).